IGM84-188-130
Etude No. 130

"LOW-CYCLE FATIGUE AND SHORT-TERM TENSILE STUDIES ON IN-265 ELEVATED TEMPERATURES"

by

Centre de Développement Technologique
École Polytechnique de Montréal

for

Industrial Materials Research Institute
National Research Council Canada

CNRC 23357

Note au lecteur:

Les idées exprimées dans ce document sont celles de l'auteur (ou du contractant) et ne sont pas nécessairement partagées par l'Institut de genie des matériaux ou par le Conseil national de recherches Canada. L'auteur (ou le contractant) en assume l'entière responsabilité.

Si la demande est suffisante, des exemplaires supplémentaires de cet ouvrage pourront être disponibles dans la seconde langue officielle (français ou anglais).

Note to the reader:

The views expressed in this document are those of the author (or contractor) who assumes their full responsibility. They are not necessarily shared by the Industrial Materials Research Institute or the National Research Council of Canada.

If sufficient requests are received, a copy of this document will be made available in the other official language (French or English).

CDT
Centre de
Développement
Technologique
École Polytechnique
de Montréal

SOMMAIRE

Ce rapport présente les résultats expérimentaux sur le comportement en fatigue uniaxiale oligocyclique pure de l'alliage à base de nickel IN 625, à des températures variant entre 482° et 816°C. Ces essais font partie d'un programme conjoint avec les essais de fatigue avec temps de maintien entrepris par IMRI/NRC, dans le but de mieux comprendre le phénomène d'interaction fatigue-fluage pour ce matériau.

Les résultats d'essais de traction sur le même matériau, à température ambiante et à haute température, sont aussi présentés.

Le rapport se termine avec quelques conclusions tirées de l'analyse préliminaire des résultats et quelques recommandations sur les travaux ultérieurs.

ACKNOWLEDGMENT

This work is part of a research project carried out in cooperation with the Industrial Materials Research Institute of NRC and Pratt and Whitney of Canada. The polished specimens have been supplied by Pratt and Whitney of Canada and the financial support has been granted by Industrial Materials Research Institute.

The assistance of Marcel Vézina in the experimental phase and the contribution of Marie Bernard-Connolly, eng. throughout the execution of this work are highly appreciated.

TABLE OF CONTENTS

	Page
SOMMAIRE	i
ACKNOWLEDGEMENT	ii
LIST OF TABLES	v
LIST OF FIGURES	vi
LIST OF SYMBOLS	viii
I. INTRODUCTION	1
II. EXPERIMENTAL PROCEDURE	2
2.1 Material and specimens	2
2.2 Testing machine	2
2.3 Specimen heating	2
2.4 Stress-strain measurements	3
2.5 Testing conditions	4
III. TEST RESULTS	5
3.1 Low cycle fatigue behavior	5
3.1.1 Variation of stress amplitude	5
3.1.2 Elastic and plastic strain ranges in terms of life	7
3.1.3 Stress-strain relationship	8
3.1.4 Fatigue curves	9
3.2 Short-term tensile behavior	13

TABLE OF CONTENTS (cont'd)

	Page
IV. CONCLUSIONS AND RECOMMENDATIONS	14
REFERENCES	17
APPENDIX A	48

LIST OF TABLES

Page

TABLE 1 - Nominal composition of IN 625 20
TABLE 2 - Test program for IN 625 21
TABLE 3 - Results of the fatigue tests on IN 625 22
TABLE 4 - Values of parameters in the relation between the elastic and plastic strain ranges with life (eq. 3.3) 28
TABLE 5a - Values of parameters in eq. 3.4 29
TABLE 5b - Values of parameters in eq. 3.5 30
TABLE 6 - Values of constants and parameters in eq. 3.7 31
TABLE 7 - Tensile properties of IN 625 32

LIST OF FIGURES

Page

FIGURE 1 - Cylindrical specimen geometry used in tests 33
FIGURE 2 - General view of testing equipment 34
FIGURE 3 - Axial extensometer mounted on specimen 34
FIGURE 4 - Variation of cyclic stress amplitude with applied cycles in fatigue tests at:
4a) 482°C 35
4b) 649°C 36
4c) 816°C 37
FIGURE 5 - Effect of temperature on the variation of the cyclic stress amplitude with applied cycles 38
FIGURE 6 - Schematic representations of the response of ductile and brittle materials under strain-controlled cycling [4] 39
FIGURE 7 - Total, elastic and plastic strain ranges versus cycles at failure for IN 625 at:
7a) 482°C 40
7b) 649°C 41
7c) 816°C 42
FIGURE 8 - Cyclic stress-strain curves for IN 625 at:
8a) 482°C 43
8b) 649°C 44
8c) 816°C 45
FIGURE 9 - Fatigue curves of IN 625 at high temperature ... 46
FIGURE 10 - Comparison of fatigue data obtained in two different laboratories at 816°C 47

LIST OF FIGURES (cont'd)

Page

FIGURES A1 to A8 - Variation of cyclic stress amplitude with applied cycles at 482°C for different strain ranges 49

FIGURES A9 to A16 - Variation of cycle stress amplitude with applied cycles at 649°C for different strain ranges 57

FIGURES A17 to A23 - Variation of cyclic stress amplitude with applied cycles at 816°C for different strain ranges 65

LIST OF SYMBOLS

a, A, b, B c, K, K', K_f n, m'	}	Material constants
E	:	Elastic modulus
N	:	Number of cycles at failure or number of applied cycles
R.A.	:	Reduction of area
Y	:	Yield strength
$\Delta\varepsilon$	:	Total strain range
$\Delta\varepsilon_e$	:	Elastic strain range
$\Delta\varepsilon_p$	:	Plastic strain range
$\dot{\varepsilon}$	:	Strain rate
$\Delta\varepsilon_o$	:	Fatigue endurance limit strain range
ε_u	:	True strain at fracture under a short-term tensile test
$\Delta\sigma$	:	Stress range
σ_u	:	Ultimate tensile stress
γ	=	$1 + \ln (\Delta\varepsilon/\Delta\varepsilon_o)$
γ_u	=	$1 + \ln (2\varepsilon_u/\Delta\varepsilon_o)$

CDT
Centre de
Développement
Technologique
École Polytechnique
de Montréal

I. INTRODUCTION

Structural components are frequently subjected to cyclic loadings at high temperatures. In particular, the nickel base superalloy IN 625 is a potential material of significant interest for such loadings in jet engines. However, little information concerning its fatigue properties is presently available and the purpose of the present report is to provide some elements of that information.

The fatigue studies were conducted jointly with IMRI/NRC; the investigations were concentrated on continuous cycling at École Polytechnique, while similar tests were performed at IMRI/NRC with the addition of hold periods in each fatigue cycle. The results obtained in both laboratories are intended to provide basic information for further study of the fatigue-creep interaction on this material at high temperatures. In addition, the influence of different test parameters, such as heating and specimen geometry, may be useful for further investigations.

II. EXPERIMENTAL PROCEDURE

2.1 Material and specimens

IN 625, specially developed for high temperature applications, is a nickel-chromium alloy strengthened by addition of molybdenum, with excellent high tensile, creep and rupture strength. The nominal composition is given in Table 1 [1].

Tests were performed on smooth cylindrical specimens with the configuration shown in Fig. 1. The specimens were supplied by Pratt and Whitney of Canada.

2.2 Testing machine

The fatigue tests were carried out using a hydraulic testing machine specially developed and built at École Polytechnique (Fig. 2). Pressure control was achieved through a hydraulic servovalve and an electronic feed-back control system [2].

2.3 Specimen heating

The specimens were resistively heated using a DC power supply with a maximum capacity of 4500 A at 4 v. The direct current is passed through the specimen by means of two water-cooled copper jackets fixed to its top and bottom parts. This set-up permits rapid heating of the specimen to the imposed temperature (for example, from room temperature to 816°C, a period of only 5 minutes is necessary).

The specimen temperature was controlled by a wrap-around chromel and alumel thermocouple. The flattened part of the thermocouple was pressed against the contour of the specimen to minimize heat losses from the junction through the thermocouple wires. The specimen temperature was maintained unchanged (± 5°C) by a feedback control system.

2.4 *Stress-strain measurements*

Stresses were measured by strain gages mounted on columns in series with the specimen. The output from these gages is sent to the control cabinet and then to the recording equipment. Strains were measured with an axial extensometer which consists of four knife edges mounted on two thin steel rings approximately 6.35 cm in diameter (Fig. 3).

The relative displacement of the knife edges mounted on the specimen is measured by two Linear Voltage Differential Transformers (LVDT). The gage length is 0.95 cm and the output signal is linear for displacements up to 0.20 cm in tension and compression, giving an approximate total strain range of 21%.

Either stress-controlled or strain-controlled fatigue tests can be achieved with either steady or variable amplitudes of stress or strain, depending on the driving signal. The frequency of loading is determined by the signal frequency.

Cyclic stress-strain hysteresis loops are periodically recorded during the life of the specimen.

Static tensile tests at different temperatures were carried out using the same test set-up.

Further details on testing procedure and equipment can be found in [2].

2.5 *Testing conditions*

The test program for evaluating the low-cycle behavior of IN 625 in air is presented in Table 2a. Test temperatures are 482°C, 649°C and 816°C and the imposed strain ranges vary between 0.4 and 2%. These parameters were selected because of a potential utilization of the material at these temperatures. The driving signal is a triangular wave form with a zero mean value and the strain rate is fixed at 10×10^{-3} s^{-1} for all tests. In addition, short-term tensile tests at the same strain rate and temperatures have been carried out as noted in Table 2b.

The variation of the cyclic stress during the life, the plastic and elastic strain components versus life and the cyclic stress-strain relationship are studied for tests under controlled strain amplitudes. In particular, the correlation between these strain components with life is examined.

III. TEST RESULTS

3.1 Low cycle fatigue behavior

A summary of the low-cycle fatigue data obtained in this study is presented in Table 3. Also included in this table are the results of some preliminary tests at 593°C (1100°F) and 704°C (1300°F), at strain ranges between 0.02 in/in and 0.005 in/in.

3.1.1 Variation of stress amplitude

The variation of the cyclic stress amplitude ($\Delta\sigma/2$) in terms of the number of applied cycles obtained at different strain ranges is summarized in Fig. 4(a), (b), (c). The details of these variations are given in Fig. A-1 to A-23 of Appendix A. At 482°C, the material cyclically hardens at all strain ranges investigated and the stabilized period is relatively small (Fig. 4a). The hardening effect is more pronounced at higher amplitudes. In particular, for $\Delta\varepsilon$ = 0.4%, the specimen initially hardens during the early stage of loading, then softens for the rest of its life.

At 649°C (Fig. 4b), the material again cyclically hardens at high strain ranges, and this hardening effect is less important at low strain ranges. Particularly, at $\Delta\varepsilon$ = 0.4%, the material behavior is relatively stable throughout its life.

At 816°C (Fig. 4c), IN 625 shows a reversed trend; in fact it cyclically softens continuously at high strain ranges. At low strain levels ($\Delta\varepsilon$ < 0.6%), a stabilization behavior throughout the life is observed.

Fig. 5 summarizes the temperature effect on the variations of the cyclic stress at three typical strain ranges. It is seen that for a given value of the strain range at the low and intermediate cycle ranges (e.g. $\Delta\varepsilon$ = 1.4% and $\Delta\varepsilon$ = 1.0%) the cyclic stress behavior is approximately the same at 482 and 649°C; however, the cyclic stresses at 816°C are significantly lower. This characteristic is less pronounced for a low strain range, i.e. $\Delta\varepsilon$ = 0.4%. In other words, the temperature effect on cyclic stress behavior is more pronounced at 816°C, especially at higher strain ranges, in comparison with that obtained for the other two temperatures.

For most specimens, the alternating stress decreases very rapidly at the end of the life. This behavior may be explained by the extension of the major fatigue crack as well as by some possible changes in the microstructure of the material. In all fatigue tests, fracture was defined as a 50% reduction of the reference cyclic stress (the usual definition in tests at École Polytechnique is a 5 reduction). In the case where there is a stabilization period, the reference cyclic stress is associated with the stabilized condition; if this is not the case, this stress is taken as the value corresponding to the beginning of a rapid drop of the curve in the diagram of $\Delta\sigma/2$ versus applied cycles.

Although the mean value of the driving strain signal is zero, a slight compressive mean stress is recorded for almost all tests (at a magnitude of 3 to 10% of the stress range $\Delta\sigma$). This is mainly due to two reasons:

(a) the nominal strain being the controlled parameter, for a given value of the maximum and minimum strain, the load required is larger in compression than in tension;

(b) in general, nickel base super alloys exhibit a greater resistance in compression than in tension [3].

3.1.2 *Elastic and plastic strain ranges in terms of life*

The hysteresis loops recorded during each test permit an evaluation of the variations of elastic and plastic strains in terms of the number of applied cycles. For IN 625, with the studied strain ranges, the width of the hysteresis loop is relatively small with respect to the total strain range; thus the elastic strain is dominant. This indicates that the material is very strong and exhibits some brittleness, as explained schematically by Fig. 6 [4].

Under completely reversed continuous strain cycling, the total strain range is usually separated into elastic and plastic components [5]:

$$\Delta\varepsilon = \Delta\varepsilon_e + \Delta\varepsilon_p \tag{3.1}$$

The elastic component $\Delta\varepsilon_e$ is determined from:

$$\Delta\varepsilon_e = \frac{\Delta\sigma}{E} \tag{3.2}$$

and the plastic component $\Delta\varepsilon_p$ is calculated using eq. (3.1).

These two components plotted in terms of the cycles at failure, are shown in Fig. 7.

Thus, with log-log coordinates, the variations of these two components may be approximated by bilinear straight lines (in some cases by a single straight line) for the three test temperatures. This may be written:

$$\Delta\varepsilon_e = AN^{-a} \tag{3.3a}$$

and

$$\Delta\varepsilon_p = BN^{-b} \tag{3.3b}$$

The values of the parameters introduced in eq. (3.3) are given in Table 4.

It should be noted that the determination of $\Delta\varepsilon_e$ in the low-strain ranges ($\Delta\varepsilon < 0.3\%$) could not be obtained with accuracy; this is due to the fact that the hysteresis loop width is relatively small and the straight part on the hysteresis loop is small.

3.1.3 *Stress-strain relationship*

Using the value of the alternating stress at half life of the specimens and the strain amplitudes (half of the total strain range), a stress-strain relationship is obtained in Fig. 8(a), 8(b) and 8(c). The correlation may be presented by a single straight line for 482°C; however for 649°C and 816°C, the bilinear behavior is more appropriate. The straight line segments are expressed by:

$$\Delta\sigma/2 = K(\Delta\varepsilon/2)^n \tag{3.4}$$

where K is a constant and n is the slope.

The values of K and n are given in Table 5a. It is observed that, for low strain ranges, the straight lines have approximately the same slope for the three test temperatures. However, at high strain ranges these slopes decrease very rapidly as the temperature increases.

Stress amplitudes in terms of the plastic strain amplitude curves are also presented in Fig. 8 for comparison purposes. Within the strain range considered, the $\Delta\sigma/2$ - $\Delta\varepsilon_p/2$ relationship may also be presented by a single straight line for 482°C; however, for 649°C and 816°C the bilinear behavior is more appropriate, as in the case of $\Delta\sigma/2$ vs $\Delta\varepsilon/2$ curves. The initial straight lines are expressed by a relation similar to eq. (3.4):

$$\Delta\sigma/2 = K'(\Delta\varepsilon_p/2)^{m'} \qquad (3.5)$$

where constants K' and m' are given in Table 5b. These curves show a trend similar to that associated with the $\Delta\sigma/2$ - $\Delta\varepsilon/2$ curves. In particular, at 816°C, for $\Delta\varepsilon_p/2 \geq 0.35\%$, m' is very small, a fact which is explained by the softening behavior of the material at 816°C, as already discussed in section 3.1.1.

3.1.4 Fatigue curves

Fatigue curves relating the total strain range $\Delta\varepsilon$ and cycles to failure N are presented in Fig. 9. Considering the isothermal curves for 482° and 649°C, it is observed that the effect of temperature on the cyclic life is approximately the same for the strain ranges investigated.

However, if we consider the curves for 482° and 816°C, this effect is more pronounced at a low strain range; for example, at $\Delta\varepsilon$ = 2% the life at 816°C, is reduced by a factor of 1.8 in comparison with the life at 482°C and this factor is about 12 at $\Delta\varepsilon$ = 0.4%. The large reduction at low strains may be attributed to the effect of time dependent processes, such as creep and oxydation, to which the material is exposed during the tests [6].

In particular, for a strain range larger than 1.2%, the fatigue life at 816°C exceeds the one at 649°C. This can be attributed to the particular characteristic of the material in the fairly low cycle region, i.e. IN 625 is cyclically hardened at 649°C but cyclically softened at 816°C (see section 3.1.1). The average fatigue curves reported in [7] for a similar material show essentially the same characteristics. Moreover, the results in [7] show that there is no regular pattern at high strain ranges.

The analysis of the fatigue results is usually made with the separation of elastic and plastic components by combining equations (3.1) and (3.3):

$$\Delta\varepsilon = AN^{-a} + BN^{-b} \tag{3.6}$$

As already noted, for a given temperature, the parameters involved in eq. (3.6) depend upon the strain range; this may give rise to some difficulties in the analysis of the creep-fatigue behavior of the material. In order to overcome this problem, the total strain is used in a cumulative fatigue damage concept recently suggested [8,9]. According to the development, the isothermal $\Delta\varepsilon$ - N curve is expressed by:

$$N = K_f \frac{1}{\gamma c} \left[\frac{1}{\gamma - 1} - \frac{1}{\gamma - (\gamma/\gamma_u)^{\sigma}} \right] \qquad (3.7)$$

where K_f and c are material constants, and γ and γ_u are the strain parameters:

$$\gamma = 1 + \ell n \, (\Delta\varepsilon/\Delta\varepsilon_o)$$

$$\gamma_u = 1 + \ell n \, (2\varepsilon_u/\Delta\varepsilon_o)$$

Constants K_f and c may be determined by referring to two data points in the $\Delta\varepsilon$ - N diagram. Fig. 9 shows the behavior of eq. (3.7) and eq. (3.6) together with the experimental results. The values of the parameters and constants introduced in eq. (3.7) are presented in Table 6.

Fig. 10 shows a comparison of fatigue data at 816°C obtained at IMRI/NRC and at École Polytechnique. For a strain range smaller than 0.9%, the fatigue life obtained at IMRI is larger than that obtained at École Polytechnique; for example, with $\Delta\varepsilon$ = 0.6%, the ratio between the two lives is of the order of 5. A reverse trend is noted for $\Delta\varepsilon$ > 0.9%.

This discrepancy between the two types of results may be related to several factors, but since it is not systematic, the exact reason is not known at this research stage. A discussion between IMRI and École Polytechnique has not lead to a definite conclusion for this purpose. Nevertheless, the following remarks may be useful concerning the specimen geometries and the heating techniques:

(a) In a previous investigation at room temperature [10] using two specimen geometries (cylindrical and hourglass specimens) with two strain measurement techniques (axial and diametral extensometers) the results

obtained under strain cycling with controlled axial strain have shown that, for a given imposed strain range, the difference in lives is relatively small (within a factor of 1.8). Thus, it seems that the discrepancy mentioned above would not be related to the specimen size effect.

Since the IMRI and École Polytechnique fatigue curves intersect, it may be possible that there are some problems concerning specimen buckling in the working section, especially for the specimen having a large value of the ratio between the cylindrical part and the diameter. This point deserves further investigations.

(b) Concerning the heating technique, the École Polytechnique specimens are heated by a direct current and exposed to the atmosphere oxydation process, whereas the IMRI specimens are heated by a radiation furnace. Thus, the latter specimens are somewhat protected from an intensive oxydation process at high temperatures. At a low strain range, due to a relatively long time of testing, this effect is more significant for École Polytechnique specimens.

It may be interesting to note here that tests have been carried out in the past, on a 304 stainless steel, using the same testing equipment [11]; the results have been compared to those reported by Berling and al [12] on a similar material. In the latter case, the hourglass specimen, heated by induction, has been used with a diametral extensometer (with the axial strain being controlled). The difference in fatigue life was systematic with a ratio of the order of 2.0 over a wide range of temperature (up to 650°C).

It is therefore suggested that the effect concerning the heating technique should be further investigated.

3.2 Short-term tensile behavior

The tensile properties of the IN 625 were determined at room temperature and at 482, 649 and 816°C. Tensile specimens had the same configuration as that of the fatigue specimens and all tensile tests were conducted using the same testing equipment. During a test, the stress was controlled to produce a nominal strain rate of 10×10^{-3} s^{-1}. Plots of stress versus strain, and stress and strain versus time were recorded.

Results of the tensile tests are summarized in Table 7. At each temperature, the results of individual tests are given along with the average value. The results are reasonably acceptable considering the experimental scatter normally expected for tensile properties, and in good agreement with data published in [13].

As expected, the strength of this alloy decreased as temperature increased; for the temperature range between 482 and 649°C, the ultimate tensile strength is approximately the same; however it decreases significantly for higher temperatures.

Concerning the yield strength, it decreases steadily with an increase of the temperature (between 482 and 816°C).

The modulus of elasticity decreases slightly when the temperature increases, as expected.

IV. CONCLUSIONS AND RECOMMENDATIONS

A study of the low cycle fatigue behavior with controlled axial strain and of the short time tensile behavior on IN 625 at high temperatures has been presented. The main conclusions are summarized as follows:

(a) IN 625 cyclically hardens at 482°C and 649°C and softens at 816°C, at high strain ranges; at low strain levels ($\Delta\varepsilon \leq 0.5\%$), however, it shows a stable behavior throughout its life in the considered temperature range.

(b) The temperature effect on cyclic stress behavior is more pronounced at 816°C, especially at high strain ranges.

(c) The elastic and plastic strain ranges versus applied cycles have been represented by bilinear expressions on a log-log plot.

(d) The stress-strain relationship has been expressed in terms of both total and plastic strain amplitudes. In both cases, at high strain ranges the slope of the straight lines decreases very rapidly as the temperature increases.

(e) Concerning the basic fatigue curves, no regular pattern has been observed at high strain ranges.

(f) The basic fatigue data can be represented by the sum of elastic and plastic components. Beside the fact that the procedure requires lengthy evaluations, parameters involved in this procedure depend upon

the strain levels considered. An alternative equation is therefore presented using the total strain range without separating into the elastic and plastic components. Satisfactory correlation with experimental results is observed.

(g) IN 625 exhibits excellent high tensile strength at room temperature, at 482° and 649°C. However, a significant decrease in strength is observed at 816°C.

The following points are suggested for future work in relation to the present study:

(a) The effect of different heating systems on fatigue life should be investigated systematically; for example, at the first stage, a few tests at room temperature at both laboratories should be carried out. The results will permit to arrive at a conclusion about the effect of heating techniques.

(b) A few tests with hold time should be carried out with the testing equipment at École Polytechnique in order to evaluate the consistency of the creep effect on the fatigue behavior, as observed in tests carried out at IMRI/NRC. The result obtained will be complementary to the experimental data of IMRI/NRC. The combined data will then be used in the analysis of the material behavior under creep-fatigue loading.

(c) The approach, developed recently at École Polytechnique [11], to estimate the life of the material subjected to a combination of fatigue/creep loading, may be a potential technique for predicting fatigue-creep life of

IN 625. In fact, this approach has been successfully applied to Alloy 800, 304 SS and 316 SS, in comparison with published experimental data [12,13].

(d) Tests with sequences of creep/fatigue (repeated sequence of a number of continuous cycles and a hold period) should be performed to study in a systematic manner the fatigue-creep interaction effect usually observed in many materials at high temperatures.

REFERENCES

1. METAL PROGRESS DATA BOOK, Metal Progress, 1975.

2. SAHEB, R.E., «A Study of the Interaction between Creep and Fatigue for an Austenitic Stainless Steel at High Temperature», D.Sc. Thesis, École Polytechnique de Montréal, July 1973.

3. STOUFFER, D.C., PAPERNIK, L., BERNSTEIN, H.L., «An Experimental Evaluation of the Mechanical Response Characteristics of René 95», Tech. Rep., AFWAL-TR-80-4136, Oct. 1980.

4. MANUAL ON LOW-CYCLE FATIGUE TESTING, ASTM STP 465, 1969.

5. BRINKMAN, C.R., BOOKER, M.K., STRIZAK, J.P. and CORWIN, W.R., «Elevated Temperature Fatigue behavior of 2 1/4 Cr-1Mo Steel», Transactions of the ASME, Jl. of Press. Vessel Tech., 1975, pp. 252-257.

6. COFFIN, L.F., «Fatigue at High Temperature», ASTM STP 520, 1973, pp. 5-36.

7. PUROHIT, A., THIELE, U., O'DONNELL, J.E., «Fatigue Strength and Evaluation of Creep Damage during Fatigue Cycling of Inconel Alloy 625», Argonne National Laboratory Report CONF-831047-14, June 1983.

8. DUBUC, J., BUI-QUOC, T., BAZERGUI, A., BIRON, A., «Unified Theory of Cumulative Damage in Metal Fatigue», Weld. Res. Concil, PVRC Bulletin 162, 1971, pp. 1-20.

9. BUI-QUOC, T., DUBUC, J., BAZERGUI, A., BIRON, A., «Cumulative Fatigue Damage under Strain Controlled Conditions», Jl. of Materials, Vol. 6, 1971, pp. 718-737.

10. BUI-QUOC, T., BIRON, A., «Comparison of Low-Cycle Fatigue Results with Axial and Diametral Extensometers», Exp. Mech., Vol. 18, 1978, pp. 127-133.

11. BUI-QUOC, T., «High Temperature Fatigue Life Estimation: Extension of a Unified Theory», Exp. Mech., Vol. 15, 1975, pp. 219-225.

12. BERLING, J.T., SLOT, T., «Effect of Temperature and Strain Rate on Low-Cycle Fatigue Resistance of AISI 304, 316 and 348 Stainless Steels», Fatigue at High Temperature, ASTM STP 459, 1969, pp. 3-30.

13. METALS HANDBOOK, ASM, 9th edition, Vol. 3, 1980.

14. BUI-QUOC, T., GOMUC, R., «A Damage Approach for Analysing the Combined Effect Under Creep-Fatigue Loading», Proc. Int. Conf. Adv. in Life Pred. Methods, ASME, Albany, April 1983, pp. 105-113.

15. GOMUC, R., «Analyse de l'effet d'interaction fatigue/fluage à haute température par une approche de dommage continu», M.Sc.A. Thesis, École Polytechnique de Montréal, August 1983.

16. GOMUC, R., BUI-QUOC, T., «An analysis of the Fatigue/Creep Behavior of 304 Stainless Steel Using a Continuous Damage Approach», to be presented at 5th International PV & P Conference, ASME, San Antonio, Texas, June 1984.

TABLE 1 - Nominal composition of IN 625, % [1]

C	Mn	Si	Cr	Mo	Cb	Ti	Al	Fe	Ni
0.05	0.25	0.25	21.5	9.0	3.65	0.2	0.2	2.5	Bal

TABLE 2 - Test program for IN 625

a) FATIGUE TESTS:

Total strain range	:	0.014, 0.012, 0.01, 0.08, 0.06, 0.04 in/in
Waveform	:	Triangular
Strain rate	:	10×10^{-3} s^{-1}
Temperature	:	482°C (900°F), 649°C (1200°F), 816°C (1500°F)
TOTAL NUMBER OF TESTS:		At each temperature three tests per strain range
		3 x 3 x 6 = 54 tests.

b) TENSILE TEST:

Temperature	:	RT, 482°C, 649°C, 816 C
Strain rate	:	10×10^{-3} s^{-1}
Replication	:	3 per temperature
TOTAL NUMBER OF TESTS:		3 x 4 = 12 tests.

TABLE 3 - Results of the Fatigue Tests on IN 625

Specimen No.	Temp. (°C)	$\dot{\varepsilon}$ (sec^{-1})	$\Delta\varepsilon$ (%)	$\Delta\varepsilon_p$ (a) (%)	$\Delta\varepsilon_e$ (%)	$\Delta\sigma$ (a) (MPa)(k)	N (b) (cycles)	Notes
7 (f)	482	10×10^{-3}	2.05	1.48	0.57	1597	305	c
11 (g)	482	10×10^{-3}	2.01	1.37	0.64	1575	330	c
27 (h)	482	10×10^{-3}	2.00	1.30	0.70	1512	462	c
32 (h)	482	10×10^{-3}	1.40	0.68	0.72	1307	996	d
50 (h)	482	10×10^{-3}	1.40	0.75	0.65	1374	943	c
53 (h)	482	10×10^{-3}	1.40	0.75	0.65	1369	993	c
33 (h)	482	10×10^{-3}	1.19	0.53	0.66	1279	1586	c
48 (h)	482	10×10^{-3}	1.19	0.57	0.62	1268	1757	d
55 (h)	482	10×10^{-3}	1.19	0.58	0.61	1268	1635	c
2 (e)	482	10×10^{-3}	0.98	0.63	0.35	1135	1825	c
16 (h)	482	10×10^{-3}	1.00	0.64	0.36	1296	2400	c
24 (h)	482	10×10^{-3}	1.00	0.65	0.35	1302	1026	d
25 (h)	482	10×10^{-3}	1.00	0.45	0.55	1204	2560	c

TABLE 3 - Results of the Fatigue Tests on IN 625

(cont'd)

Specimen No.	Temp. (°C)	$\dot{\varepsilon}$ (sec^{-1})	$\Delta\varepsilon$ (%)	$\Delta\varepsilon_p$ (a) (%)	$\Delta\varepsilon_e$ (%)	$\Delta\sigma$ (a) (MPa)(k)	N (b) (cycles)	Notes
46 (h)	482	10×10^{-3}	1.00	0.42	0.58	1175	1790	c
56 (h)	482	10×10^{-3}	1.00	0.43	0.57	1221	1350	c
34 (h)	482	10×10^{-3}	0.80	0.28	0.52	950	2400	c
44 (h)	482	10×10^{-3}	0.80	0.27	0.53	1025	5888	c
59 (h)	482	10×10^{-3}	0.80	0.30	0.50	960	3790	c
65 (h)	482	10×10^{-3}	0.80	0.30	0.50	960	3590	c
35 (h)	482	10×10^{-3}	0.60	0.16	0.44	840	6747	c
43 (h)	482	10×10^{-3}	0.60	0.13	0.47	873	7947	d
60 (h)	482	10×10^{-3}	0.60	--	--	--	--	j
61 (h)	482	10×10^{-3}	0.60	0.16	0.44	915	4400	c
6 (f)	482	5×10^{-3}	0.49	0.16	0.33	949	27300	c
13 (h)	482	10×10^{-3}	0.50	0.28	0.22	990	17007	d
28 (h)	482	10×10^{-3}	0.50	0.11	0.39	810	8700	c
36 (h)	482	8×10^{-3}	0.40	0.027	0.37	730	92160	i
66 (h)	482	8×10^{-3}	0.40	0.10	0.30	728	25939	c
68 (h)	482	8×10^{-3}	0.40	0.10	0.30	738	54821	d

TABLE 3 - Results of the Fatigue Tests on IN 625

(cont'd)

Specimen No.	Temp. (°C)	$\dot{\varepsilon}$ (sec^{-1})	$\Delta\varepsilon$ (%)	$\Delta\varepsilon_p$ (a) (%)	$\Delta\varepsilon_e$ (%)	$\Delta\sigma$ (a) (MPa)(k)	N (b) (cycles)	Notes
10 (g)	593	10×10^{-3}	2.01	1.50	0.51	1620	122	c
21 (h)	593	10×10^{-3}	2.01	1.50	0.51	1633	150	d
4 (f)	593	10×10^{-3}	1.00	0.58	0.42	1186	1280	c
9 (g)	593	10×10^{-3}	1.00	0.72	0.28	1240	741	c
23 (h)	593	10×10^{-3}	1.00	0.71	0.29	1280	745	c
8 (g)	593	10×10^{-3}	0.51	0.34	0.17	782	3369	c
15 (h)	593	10×10^{-3}	0.50	0.32	0.18	785	4490	c
22 (h)	593	10×10^{-3}	0.50	0.34	0.16	855	2540	c
31 (h)	649	10×10^{-3}	2.01	1.19	0.82	1493	194	d
37 (h)	649	10×10^{-3}	1.40	0.75	0.65	1406	300	e
51 (h)	649	10×10^{-3}	1.40	0.69	0.71	1389	407	c
52 (h)	649	10×10^{-3}	1.40	0.68	0.72	1418	413	d
38 (h)	649	10×10^{-3}	1.19	0.66	0.53	1230	417	d
49 (h)	649	10×10^{-3}	1.19	0.64	0.55	1224	513	c
54 (h)	649	10×10^{-3}	1.19	0.57	0.62	1169	640	c
30 (h)	649	10×10^{-3}	1.00	0.45	0.55	1131	767	c
47 (h)	649	10×10^{-3}	1.00	0.48	0.52	1149	817	c

TABLE 3 - Results of the Fatigue Tests on IN 625
(cont'd)

Specimen No.	Temp. (°C)	$\dot{\varepsilon}$ (sec^{-1})	$\Delta\varepsilon$ (%)	$\Delta\varepsilon_p$ (a) (%)	$\Delta\varepsilon_e$ (%)	$\Delta\sigma$ (a) (MPa)(k)	N (b) (cycles)	Notes
57 (h)	649	10×10^{-3}	1.00	0.47	0.53	1107	537	d
39 (h)	649	10×10^{-3}	0.80	0.32	0.48	949	1416	c
45 (h)	649	10×10^{-3}	0.80	0.45	0.35	942	1332	c
58 (h)	649	10×10^{-3}	0.80	0.31	0.49	926	1130	c
40 (h)	649	10×10^{-3}	0.60	0.17	0.43	729	1500	c
41 (h)	649	10×10^{-3}	0.60	0.16	0.44	810	1749	c
42 (h)	649	10×10^{-3}	0.60	0.17	0.43	779	2050	c
62 (h)	649	10×10^{-3}	0.51	0.12	0.39	668	2648	c
63 (h)	649	10×10^{-3}	0.51	0.15	0.36	736	3900	c
64 (h)	649	10×10^{-3}	0.51	0.14	0.37	722	5122	c
67 (h)	649	8×10^{-3}	0.40	0.10	0.30	665	46325	i
69 (h)	649	8×10^{-3}	0.40	0.10	0.30	650	8542	c
91 (h)	649	8×10^{-3}	0.40	0.05	0.35	650	19081	c
14 (h)	704	10×10^{-3}	2.01	1.46	0.55	1442	145	d
19 (h)	704	10×10^{-3}	2.01	1.48	0.53	1400	230	c
5 (f)	704	10×10^{-3}	0.99	0.58	0.41	1134	593	c
17 (h)	704	10×10^{-3}	1.00	0.68	0.32	1198	479	c
20 (h)	704	10×10^{-3}	1.00	0.70	0.30	1192	290	c
12 (g)	704	10×10^{-3}	0.51	0.29	0.22	728	3765	c
18 (h)	704	10×10^{-3}	0.50	0.31	0.10	759	6873	c

TABLE 3 - Results of the Fatigue Tests on IN 625
(cont'd)

Specimen No.	Temp. (°C)	$\dot{\varepsilon}$ (sec^{-1})	$\Delta\varepsilon$ (%)	$\Delta\varepsilon_p$ (a) (%)	$\Delta\varepsilon_e$ (%)	$\Delta\sigma$ (a) (MPa)(k)	N (b) (cycles)	Notes
81 (h)	816	10×10^{-3}	2.00	1.46	0.54	872	250	c
75 (h)	816	10×10^{-3}	1.4	0.95	0.45	872	456	d
77 (h)	816	10×10^{-3}	1.4	0.97	0.43	852	434	c
90 (h)	816	10×10^{-3}	1.4	0.95	0.45	900	385	c
74 (h)	816	10×10^{-3}	1.19	0.74	0.45	850	383	d
82 (h)	816	10×10^{-3}	1.19	0.74	0.45	854	536	c
89 (h)	816	10×10^{-3}	1.19	0.73	0.46	890	510	c
70 (h)	816	10×10^{-3}	1.00	0.58	0.42	830	574	c
71 (h)	816	10×10^{-3}	1.00	0.59	0.41	856	502	d
88 (h)	816	10×10^{-3}	1.00	0.54	0.46	792	456	c
72 (h)	816	10×10^{-3}	0.80	0.47	0.33	744	547	d
83 (h)	816	10×10^{-3}	0.80	0.40	0.40	692	1040	c
87 (h)	816	10×10^{-3}	0.80	0.42	0.38	722	680	c
78 (h)	816	10×10^{-3}	0.60	0.30	0.30	660	689	c
79 (h)	816	10×10^{-3}	0.60	0.27	0.33	632	924	c
86 (h)	816	10×10^{-3}	0.60	0.27	0.33	610	924	d

TABLE 3 - Results of the Fatigue Tests on IN 625
(cont'd)

Specimen No.	Temp. (°C)	$\dot{\varepsilon}$ (sec^{-1})	$\Delta\varepsilon$ (%)	$\Delta\varepsilon_p$ (a) (%)	$\Delta\varepsilon_e$ (%)	$\Delta\sigma$ (a) (MPa)(k)	N (b) (cycles)	Notes
80 (h)	816	8×10^{-3}	0.40	0.10	0.30	496	2202	c
84 (h)	816	8×10^{-3}	0.40	0.10	0.30	482	3880	d
85 (h)	816	8×10^{-3}	0.40	0.09	0.31	498	5330	c

Notes:
(a) Determined at N/2
(b) Number of cycles corresponding to a reduction of 50% of the stabilized cyclic stress
(c) Crack initiated inside the gage length
(d) Crack initiated outside the gage length
(e) Surface finished by P & W
(f) Surface finished by École Polytechnique
(g) Surface finished by P & W (2nd series)
(h) Surface finished P & W (3rd series)
(i) Test stopped intentionally when cyclic life for exceeded expected behavior
(j) Test stopped because of manipulation errors
(k) Conversion factor 1 ksi = 6.89 MPa

TABLE 4 - Values of parameters in the relation between the elastic and plastic strain ranges with life (eq. 3.3)

Temp. (°C)	Temp. (°F)	A	a	B	b	Range of life (cycles)
482	900	0.034	0.232	2.19	0.835	$400 \leq N \leq 10000$
482	900	0.034	0.232	0.001	0.0	$10000 \leq N \leq 60000$
649	1200	0.031	0.257	0.422	0.683	$150 \leq N \leq 8000$
649	1200	0.004	0.019	0.422	0.683	$8000 \leq N \leq 50000$
816	1500	0.023	0.259	16.45	1.259	$200 \leq N \leq 2000$
816	1500	0.004	0.032	16.45	1.259	$2000 \leq N \leq 2200$
816	1500	0.004	0.032	0.002	0.107	$2200 \leq N \leq 6000$

TABLE 5a - Values of parameters in eq. (3.4)

Temp. (°C)	Temp. (°F)	K (MPa)	n	Range of strain
482	900	7094	0.474	$0.002 < \Delta\varepsilon/2 \leq 0.01$
649	1200	11818	0.579	$\Delta\varepsilon/2 \leq 0.007$
649	1200	2882	0.291	$0.007 < \Delta\varepsilon/2$
816	1500	8245	0.564	$\Delta\varepsilon/2 \leq 0.0052$
816	1500	558	0.049	$0.0052 < \Delta\varepsilon/2$

TABLE 5b - Values of parameters in eq. (3.5)

Temp. (°C)	Temp. (°F)	K' (MPa)	m'	Range of plastic strain
482	900	2788	0.254	$0.0005 \leq \Delta\varepsilon_p/2 \leq 0.0075$
649	1200	9540	0.465	$\Delta\varepsilon_p/2 \leq 0.0035$
649	1200	1955	0.186	$0.0035 \leq \Delta\varepsilon_p/2$
816	1500	3890	0.381	$\Delta\varepsilon_p/2 \leq 0.003$
816	1500	565	0.047	$0.003 \leq \Delta\varepsilon_p/2$

TABLE 6 - Values of constants and parameters in eq. (3.7)

Temp. (°C)	Temp. (°F)	$\Delta\varepsilon_o$ (%)	ε_u (%)	K_f	a
482	900	0.30	63.0	20060	1.86
649	1200	0.30	100.2	4625	1.34
816	1500	0.23	126.0	1882	0.004

TABLE 7 - Tensile properties of IN 625 (with $\dot{\varepsilon} = 10 \times 10^{-3}\ s^{-1}$)

Specimen No.	Temperature (°C)	(°F)	E (kSi)	(GPa)	Y (kSi)	(MPa)	σ_u (kSi)	(MPa)	RA (%)	ε_u (%)
92	R.T.	R.T.	-	-	-	-	139.5	961	51.6	72.5
93			29400	202	85.5	589	135.5	934	-	-
94			29500	203	87.0	599	139.1	958	49.5	68.3
95			29200	201	82.0	565	139.2	959	48.4	66.2
Average			29300	202	84.8	585	138.3	953	49.8	68.9
96	482	900	27200	287	59.4	409	114.9	792	42.3	54.9
97			26800	185	61.5	424	128.3	384	48.9	67.3
98			29300	202	55.5	382	94.5	651	46.9	63.3
105			28100	194	57.5	396	97.5	671	48.6	66.6
Average			27900	192	58.5	403	108.8	749	46.7	62.9
99	649	1200	27600	190	51.0	351	107.3	739	63.3	100.2
100			29700	205	53.2	367	108.7	749	63.1	99.7
101			24600	169	51.0	351	105.0	723	63.5	100.7
Average			27300	188	51.7	356	107.0	737	63.3	100.2
102	816	1500	24200	167	52.5	362	76.5	527	69.9	120.2
103			23600	163	49.5	341	71.3	491	64.0	102.2
104			22100	152	49.1	338	72.8	501	80.9	165.5
Average			23300	161	50.3	347	73.5	507	71.6	126.0

	Dimensions	
	mm	po
ϕ_1	22.99	0.905
ϕ_2	12.83	0.505
L	165.10	6.50
L_1	19.05	0.75
L_2	25.40	1.00
L_3	24.13	0.95
L_4	15.24	0.60
L_5	31.75	1.25

Cylindrical part;
Length L_4 Dia. ϕ_2

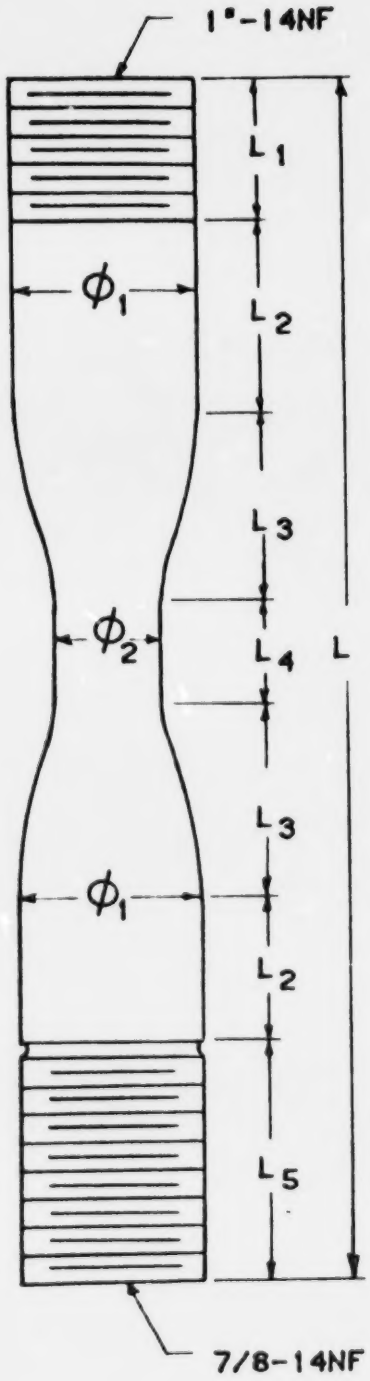

FIG. 1 - Cylindrical specimen geometry used in tests.

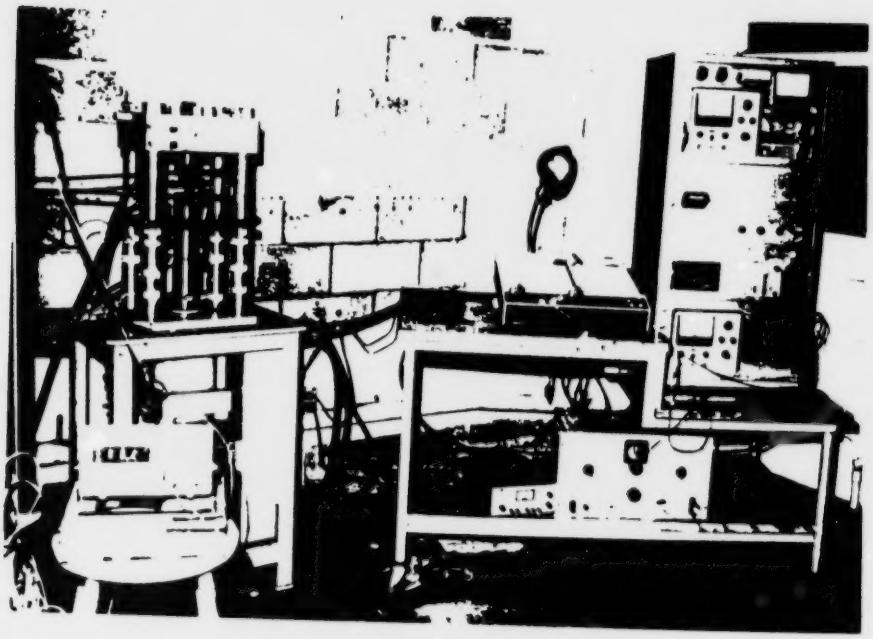

FIG. 2 - General view of testing equipment.

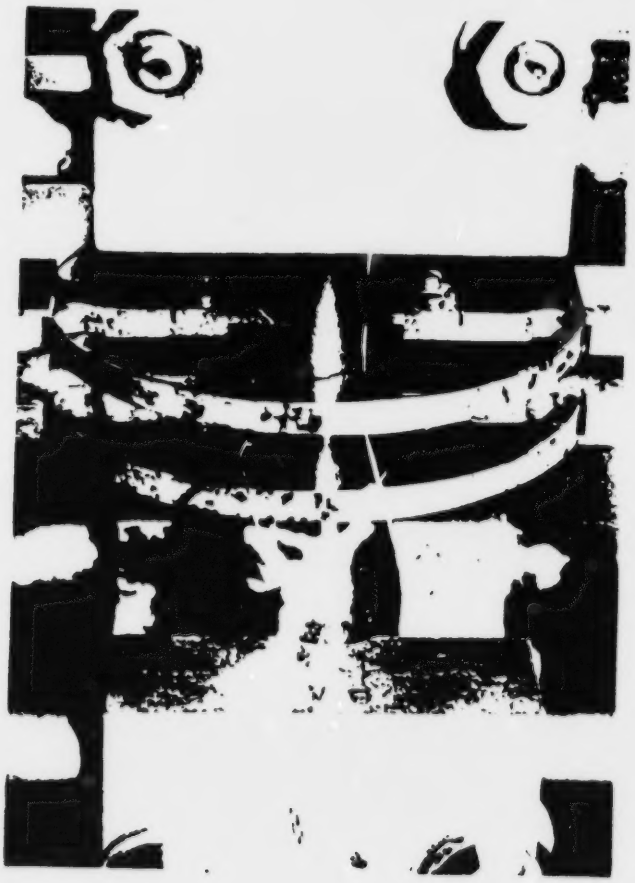

FIG. 3 - Axial extensometer mounted on specimen.

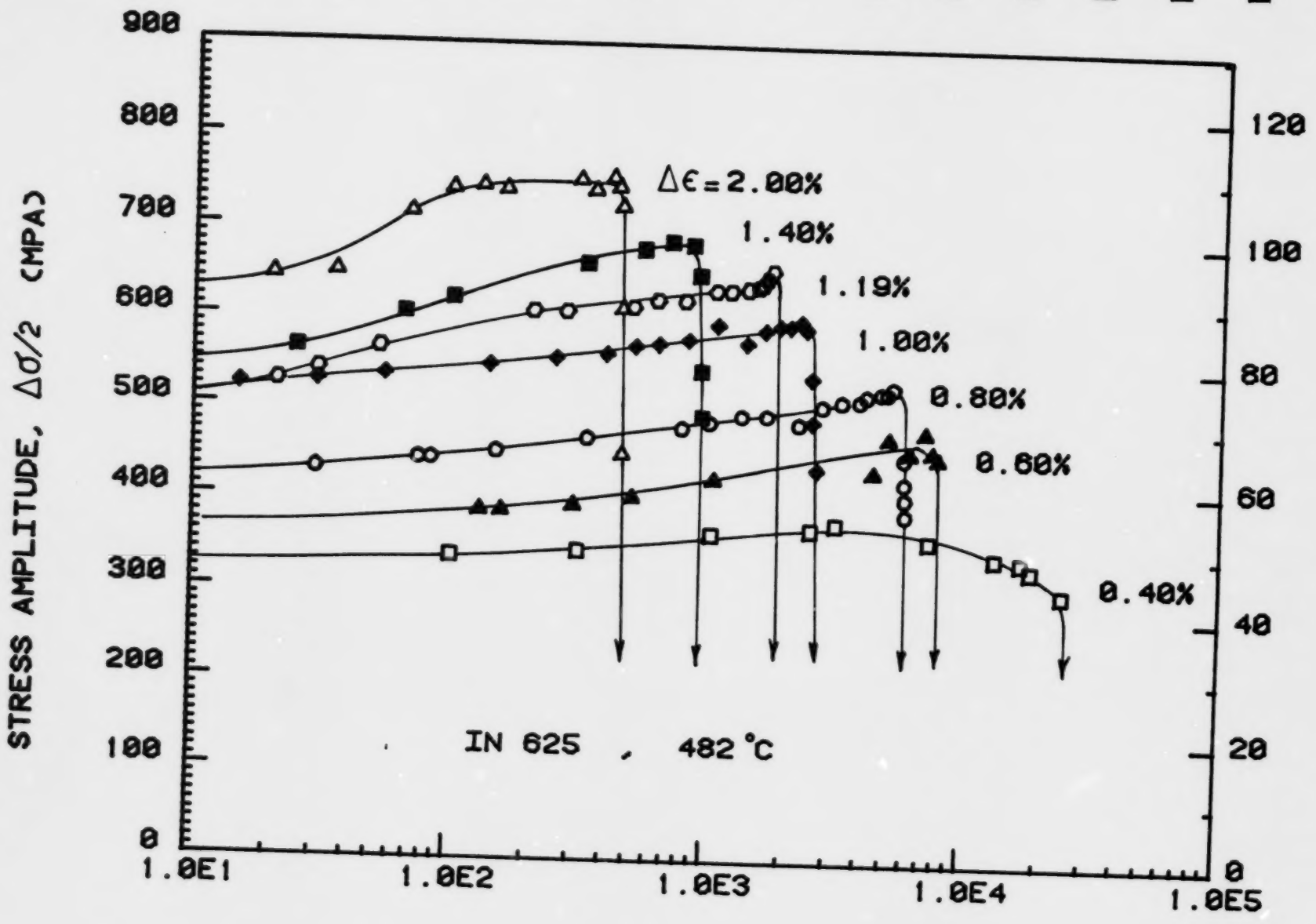

FIG. 4a - Variation of cyclic stress amplitude with applied cycles at 482°C.

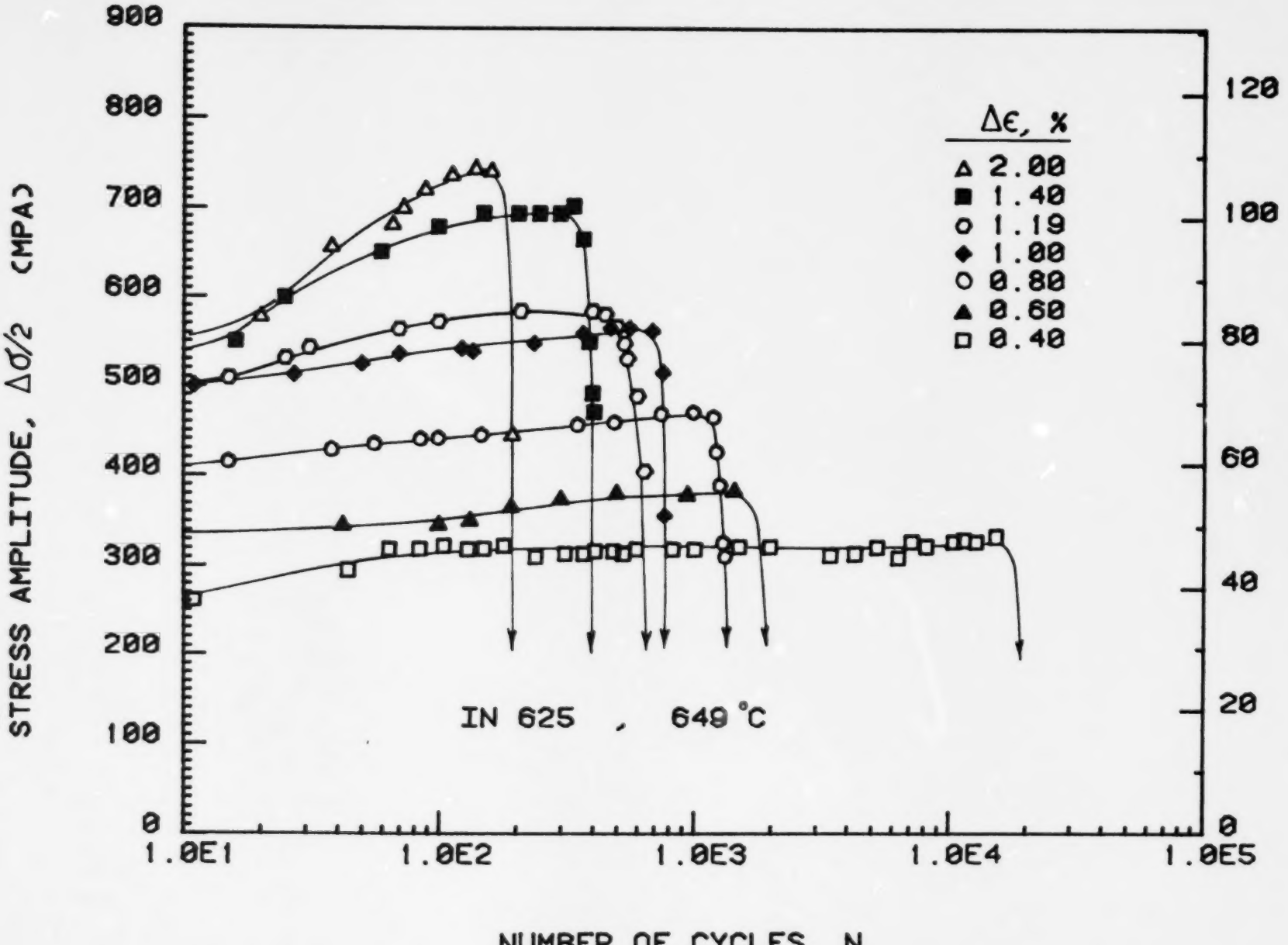

FIG. 4b - Variation of cyclic stress amplitude with applied cycles at 649°C.

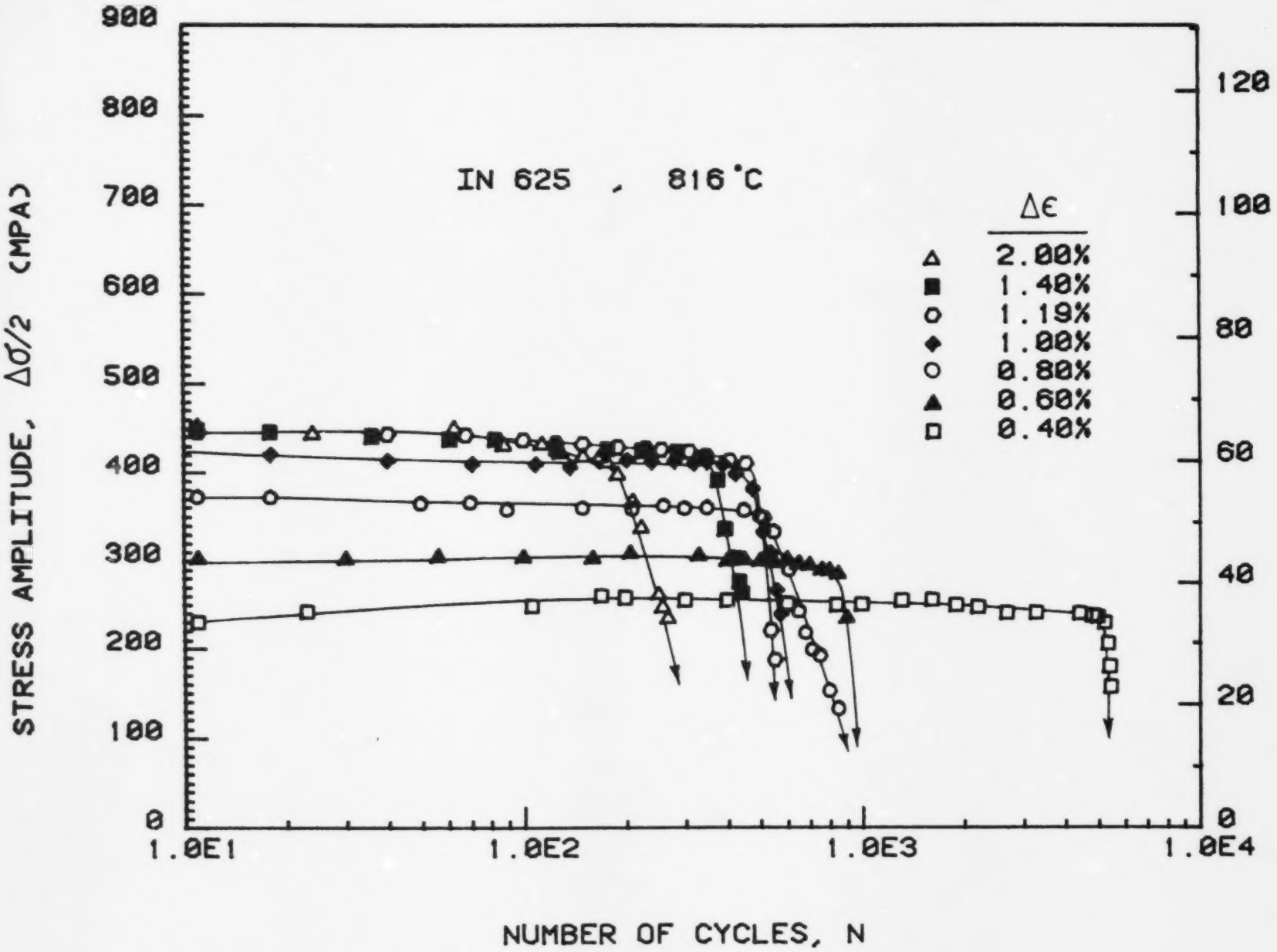

FIG. 4c - Variation of cyclic stress amplitude with applied cycles at 816°C.

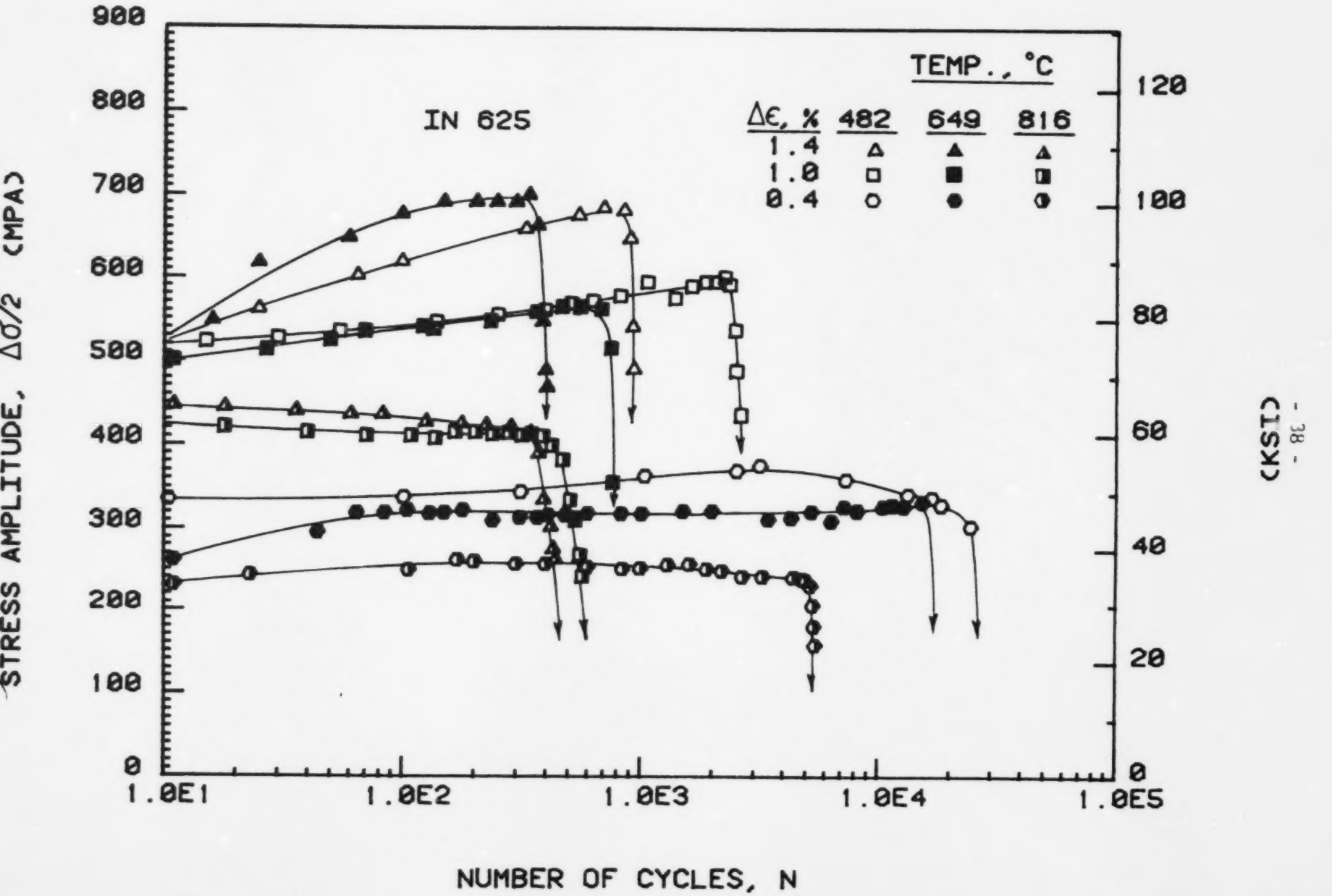

FIGURE 5 - Effect of temperature on the variation of the cyclic stress amplitude with applied cycles.

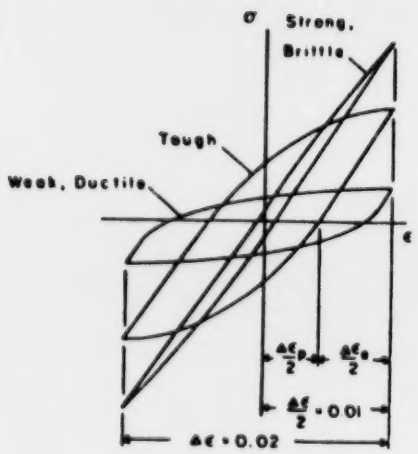

FIG. 6 - Schematic representations of the response of ductile and brittle materials under strain-controlled cycling [4].

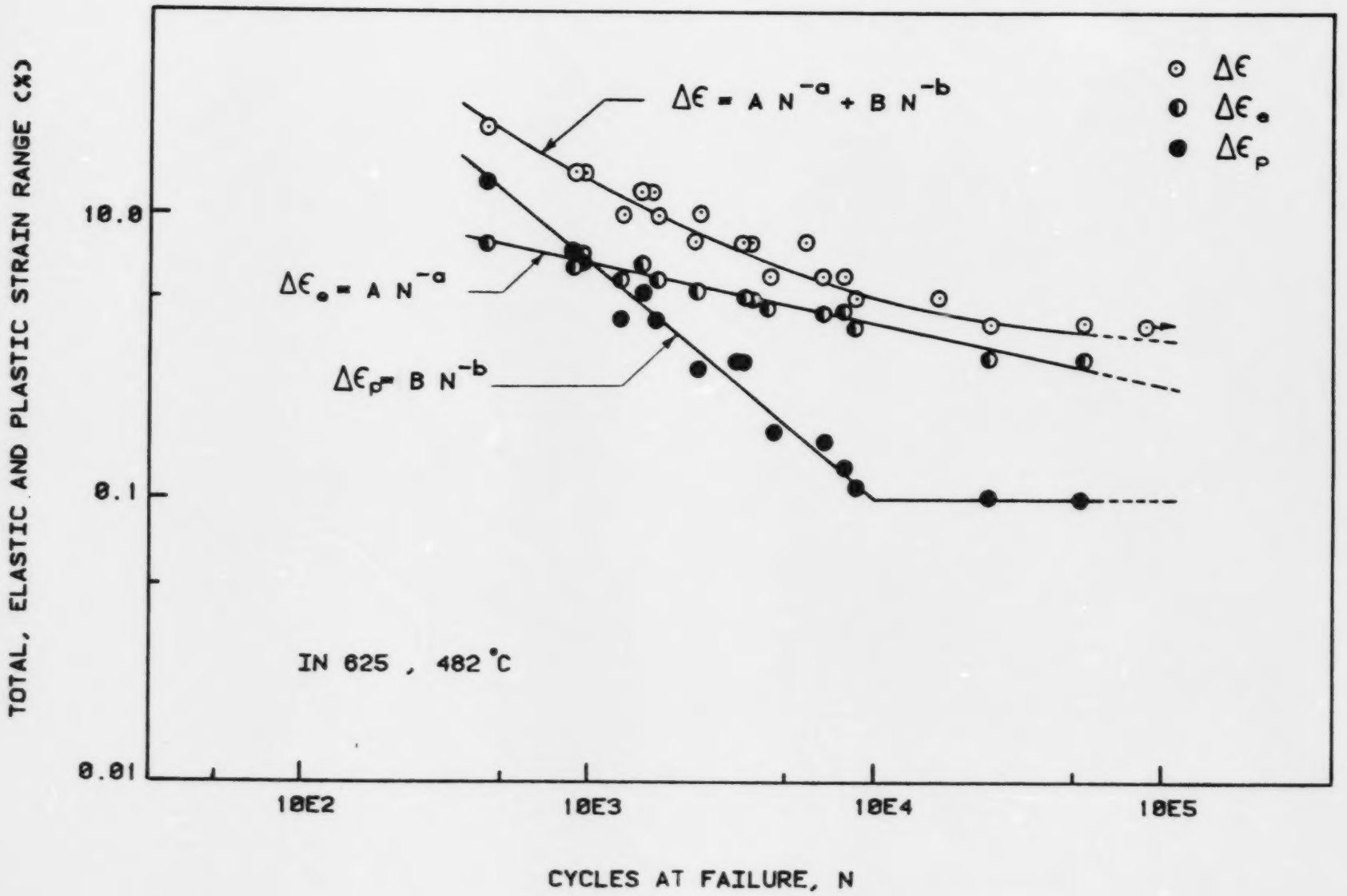

FIG. 7a - Total, elastic and plastic strain ranges versus cycles at failure for IN 625 at 482°C.

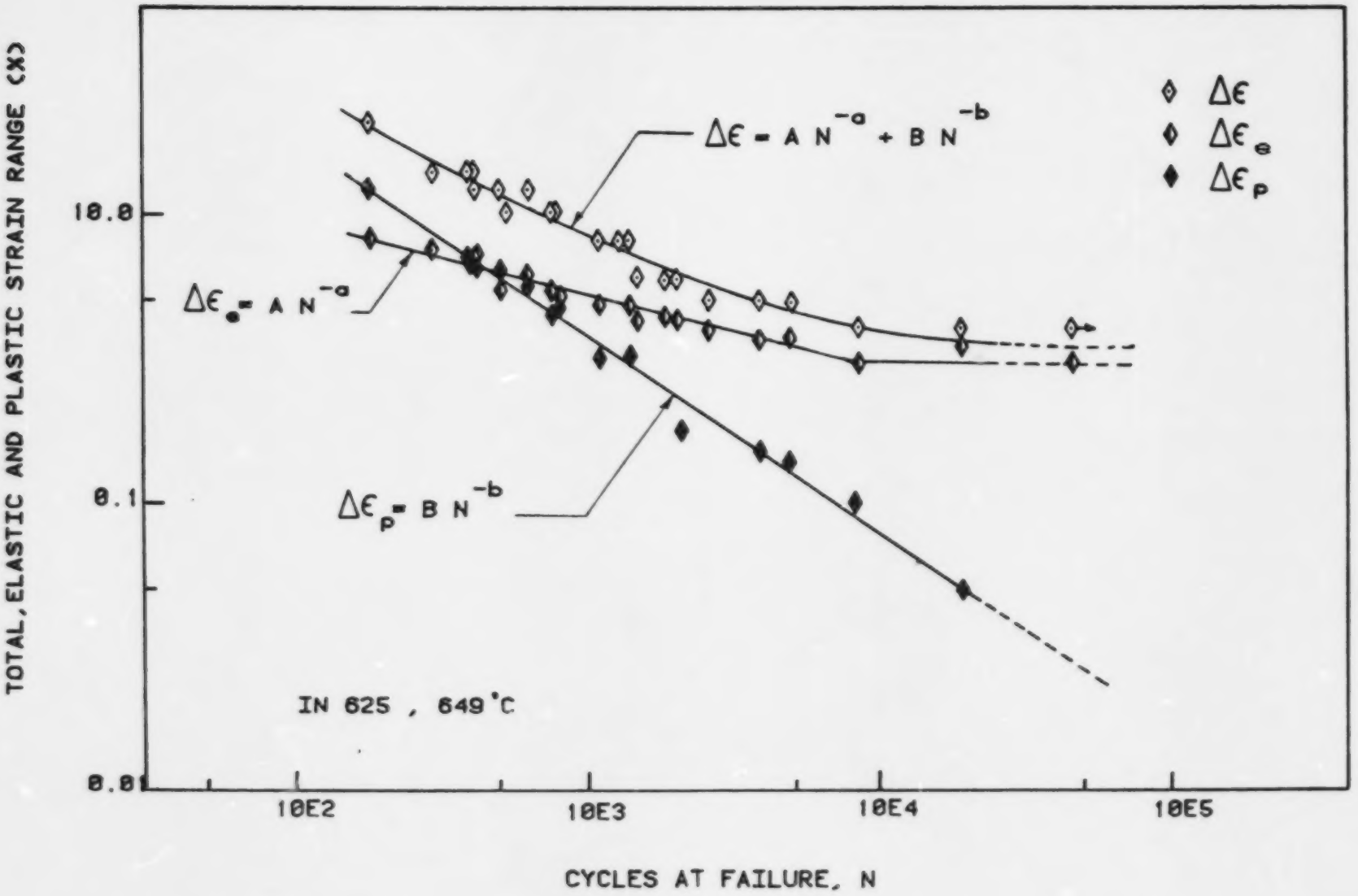

FIG. 7b - Total, elastic and plastic strain ranges versus cycles at failure for IN 625 at 649°C.

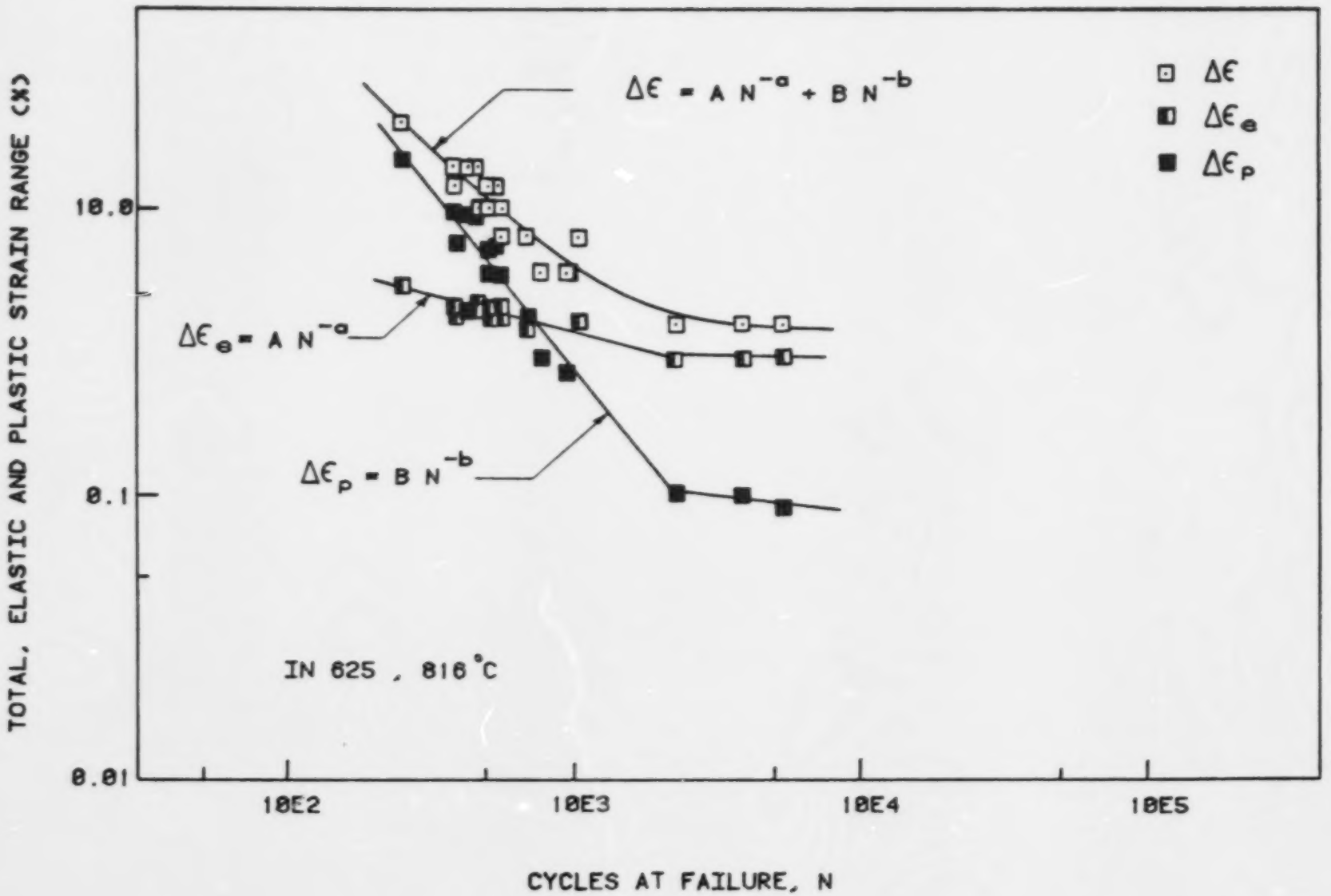

FIG. 7c - Total, elastic and plastic strain ranges versus cycles at failure for IN 625 at 816°C.

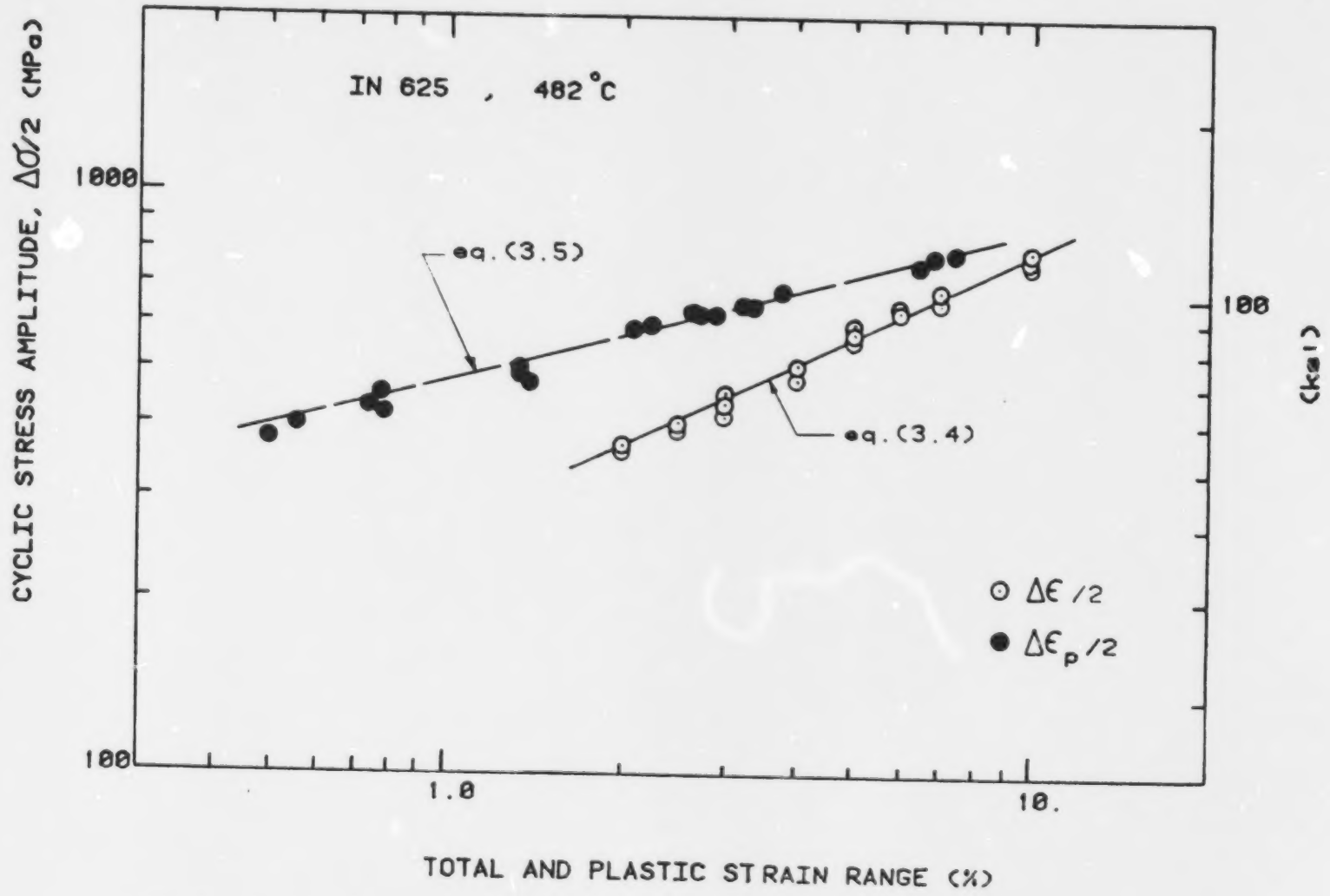

FIG. 8a - Cyclic stress-strain curves for IN 625 at 482°C.

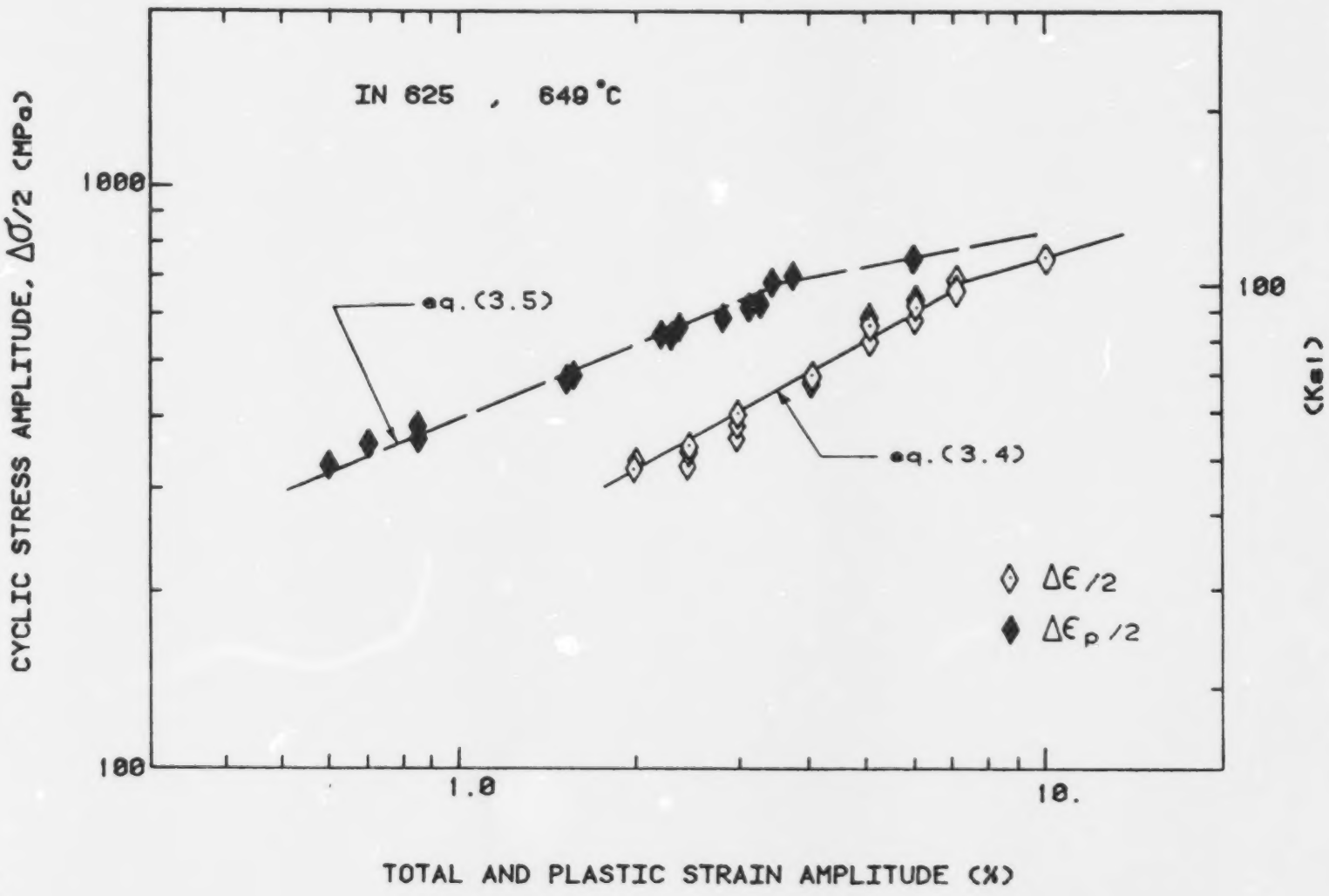

FIG. 8b - Cyclic stress-strain curves for IN 625 at 649°C.

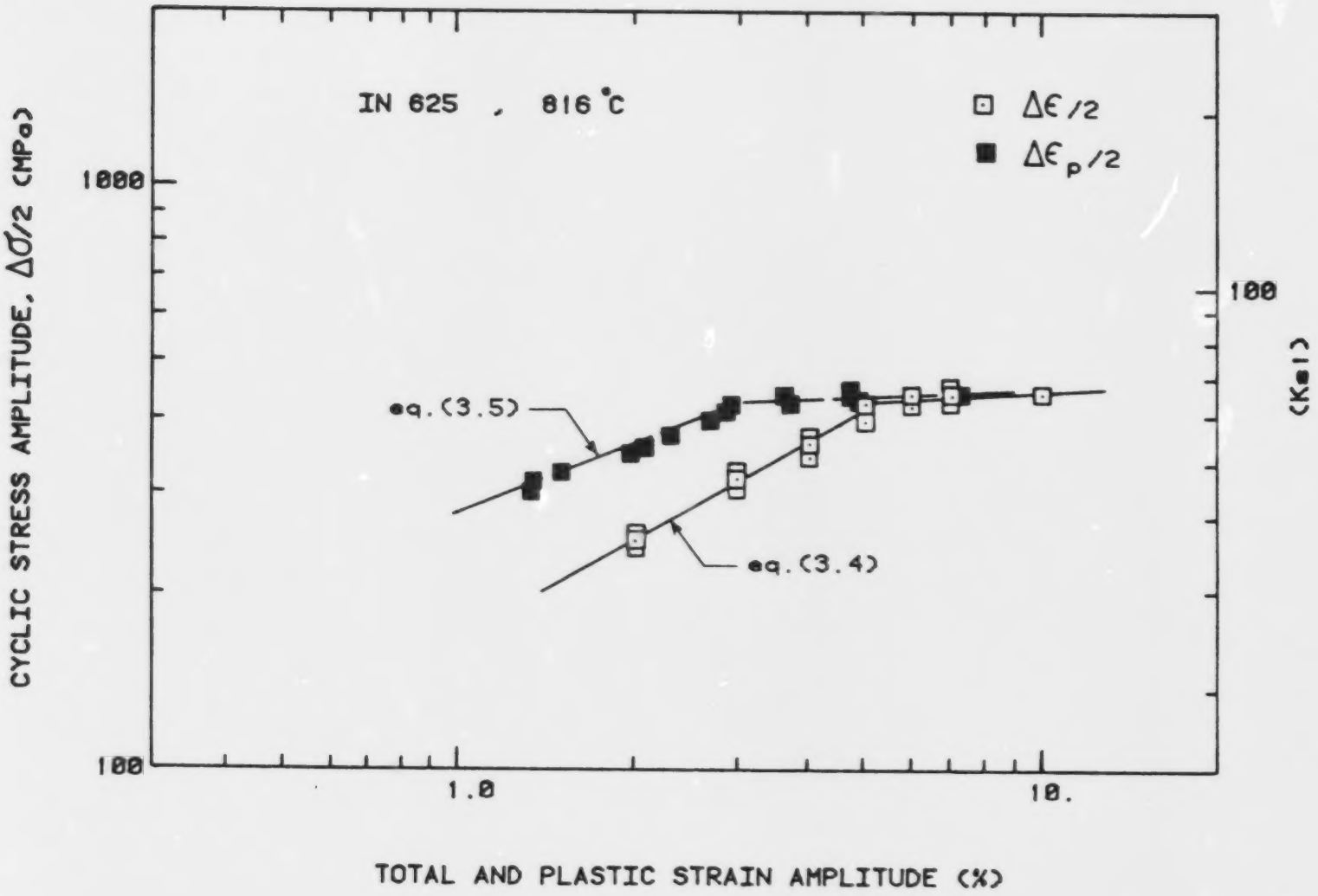

FIG. 8c - Cyclic stress-strain curves for IN 625 at 816°C.

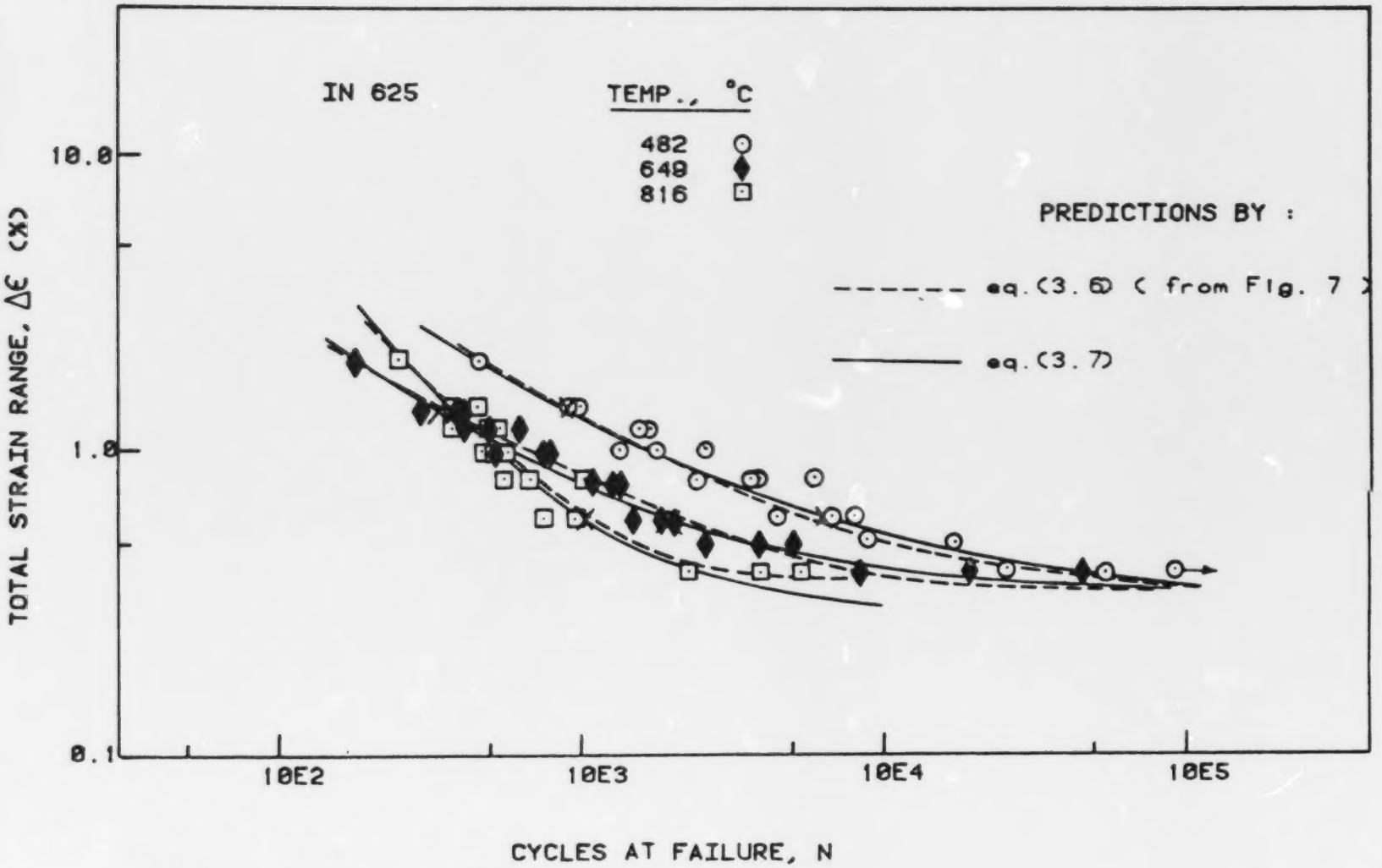

FIG. 9 - Fatigue curves of IN 625 at high temperature.

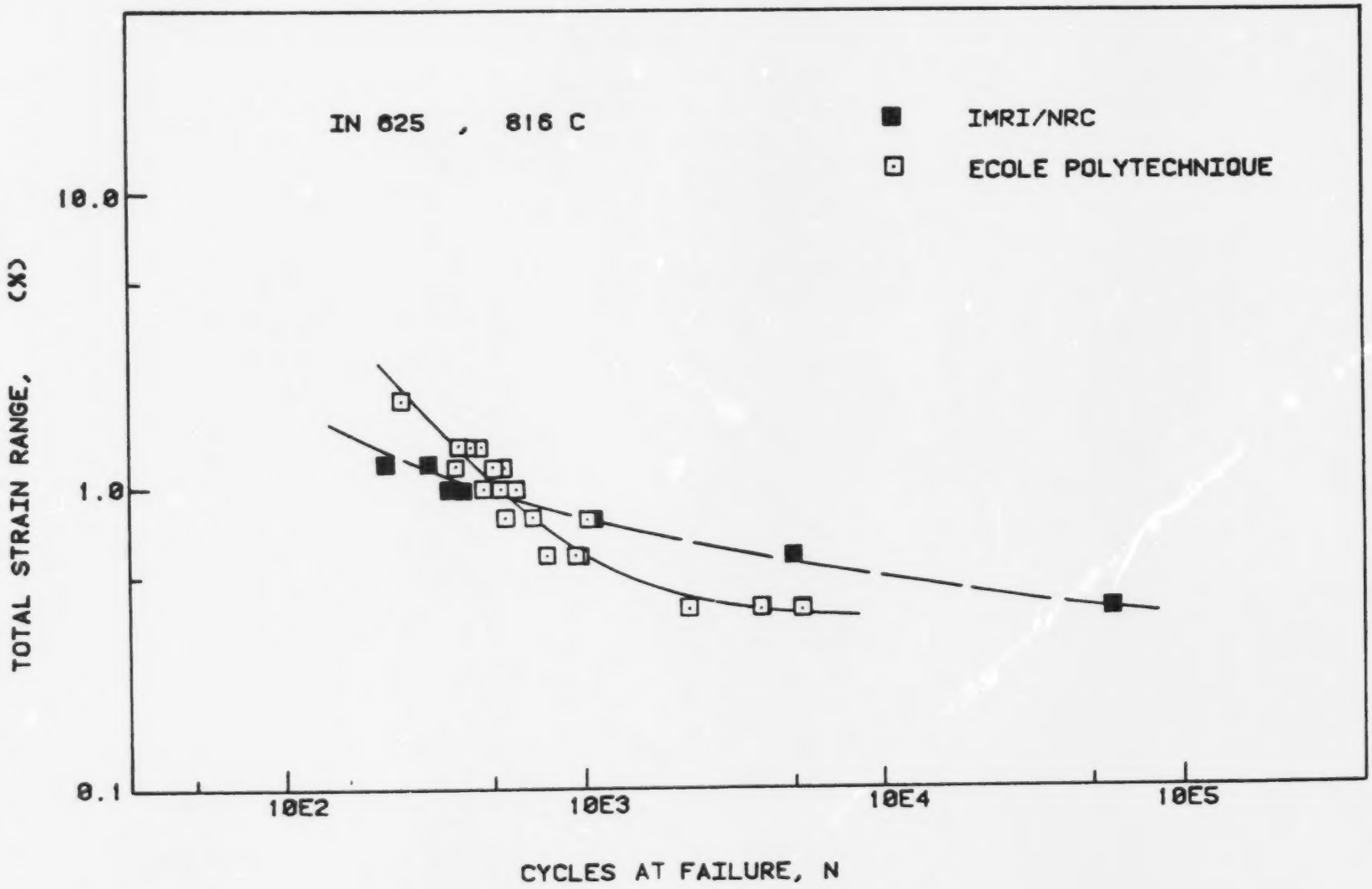

FIG. 10 - Comparison of fatigue data obtained in two different laboratories at 816°C.

APPENDIX A

Cyclic stress amplitude versus
applied cycles curves

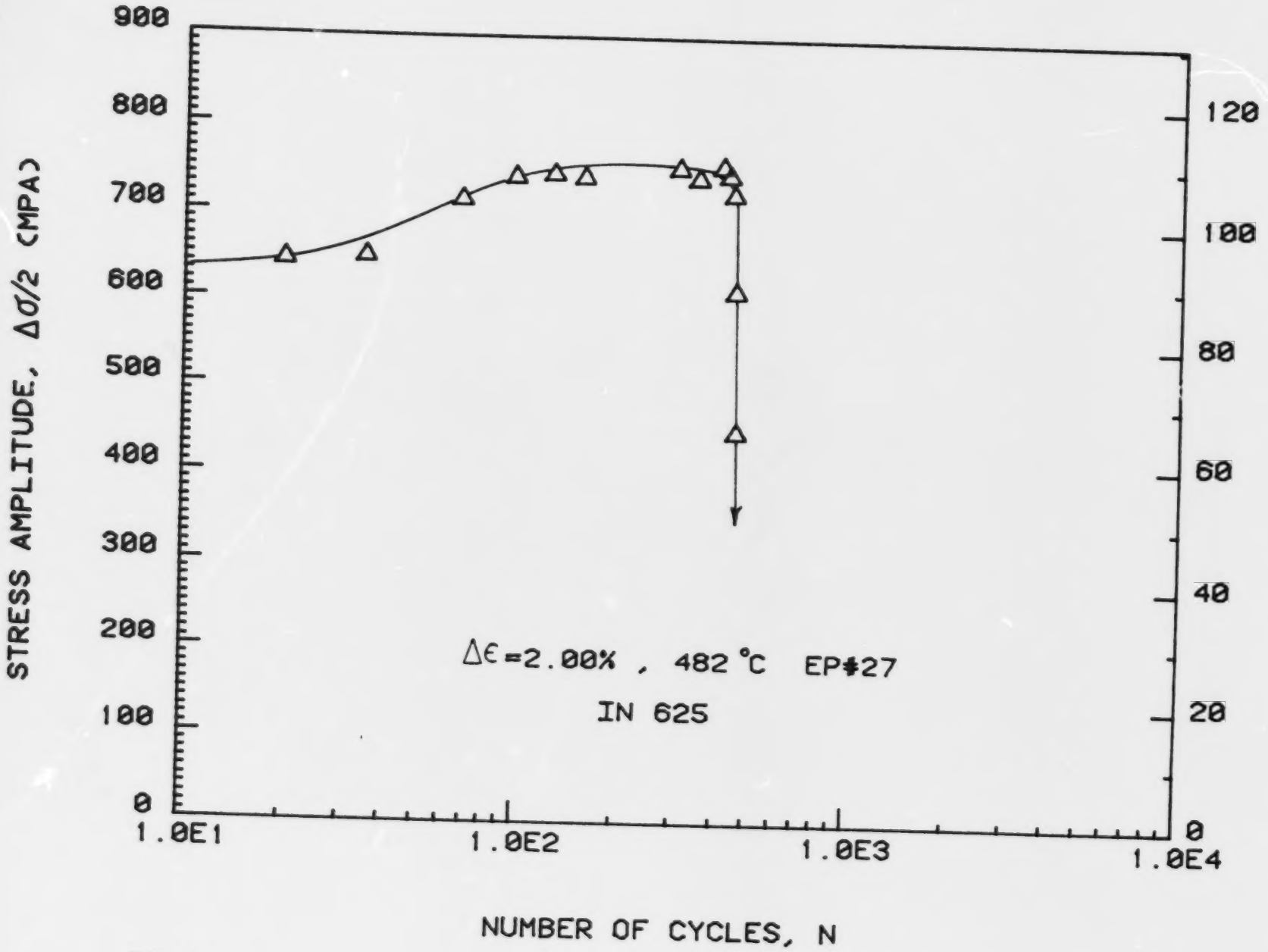
900
800
700
600
500
400
300
200
100
0
STRESS AMPLITUDE, Δσ/2 (MPA)
120
100
80
60
40
20
0
(KSI)
Δε=2.00% , 482 °C EP#27
IN 625
1.0E1
1.0E2
1.0E3
1.0E4
NUMBER OF CYCLES, N

FIG. A.1

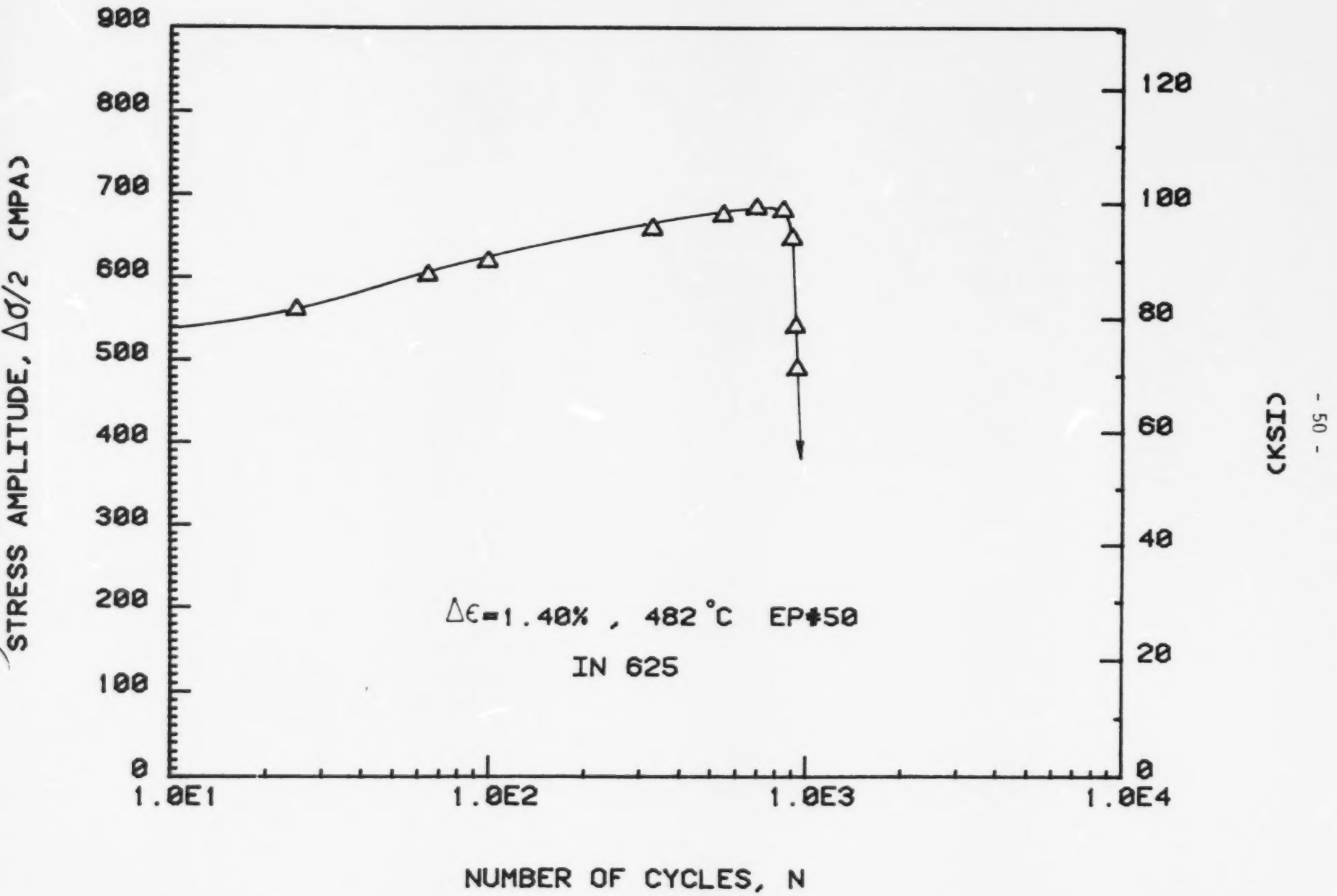
900
800
700
600
500
400
300
200
100
0
120
100
80
60
40
20
0
1.0E1
1.0E2
1.0E3
1.0E4
STRESS AMPLITUDE, Δσ/2 (MPA)
(KSI)
Δε=1.40% , 482 °C EP#50
IN 625
NUMBER OF CYCLES, N

FIG. A.2

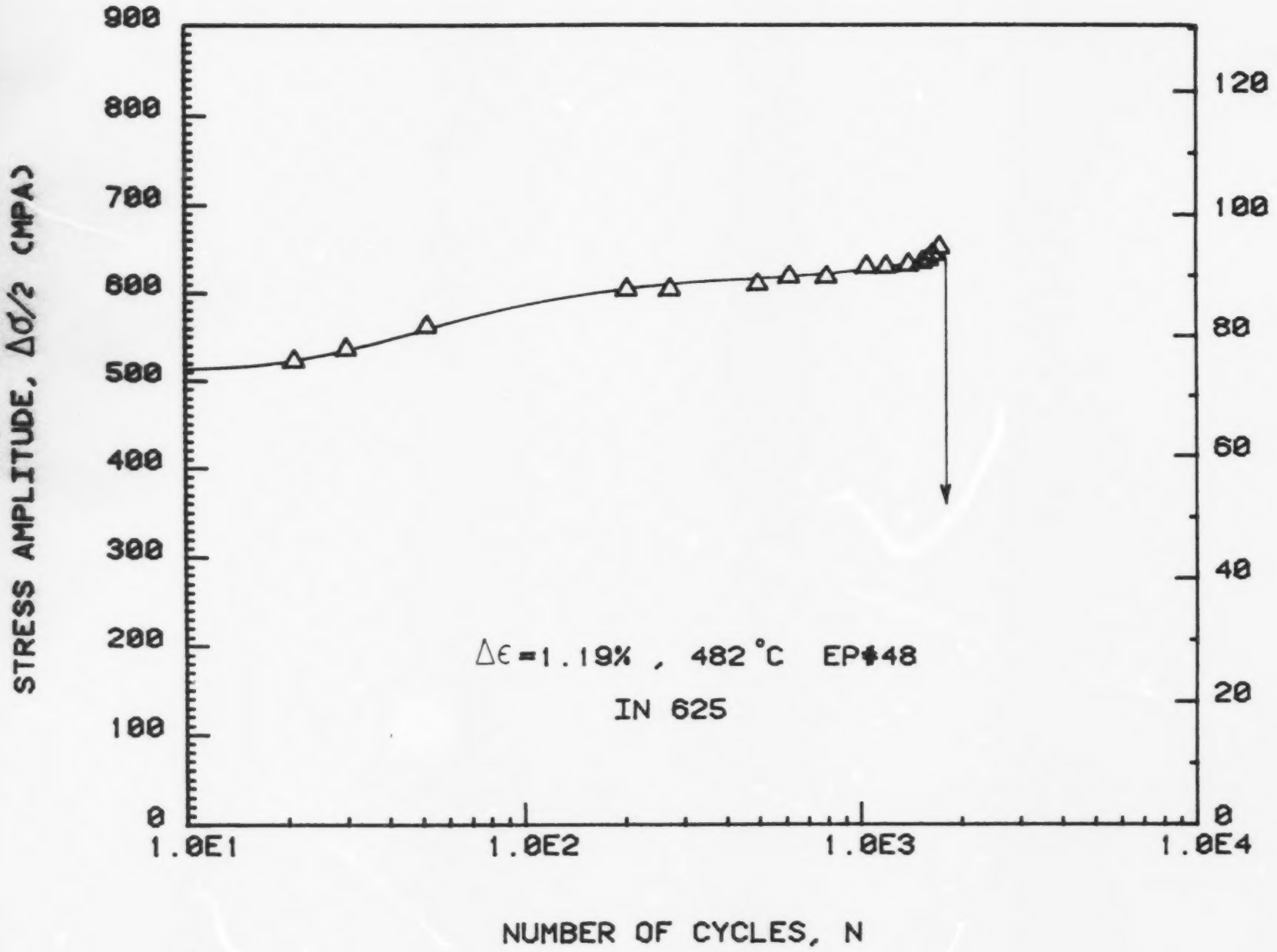
900
800
700
600
500
400
300
200
100
0
120
100
80
60
40
20
0
1.0E1
1.0E2
1.0E3
1.0E4
STRESS AMPLITUDE, Δσ/2 (MPA)
(KSI)
Δε=1.19% , 482°C EP#48
IN 625
NUMBER OF CYCLES, N

FIG. A.3

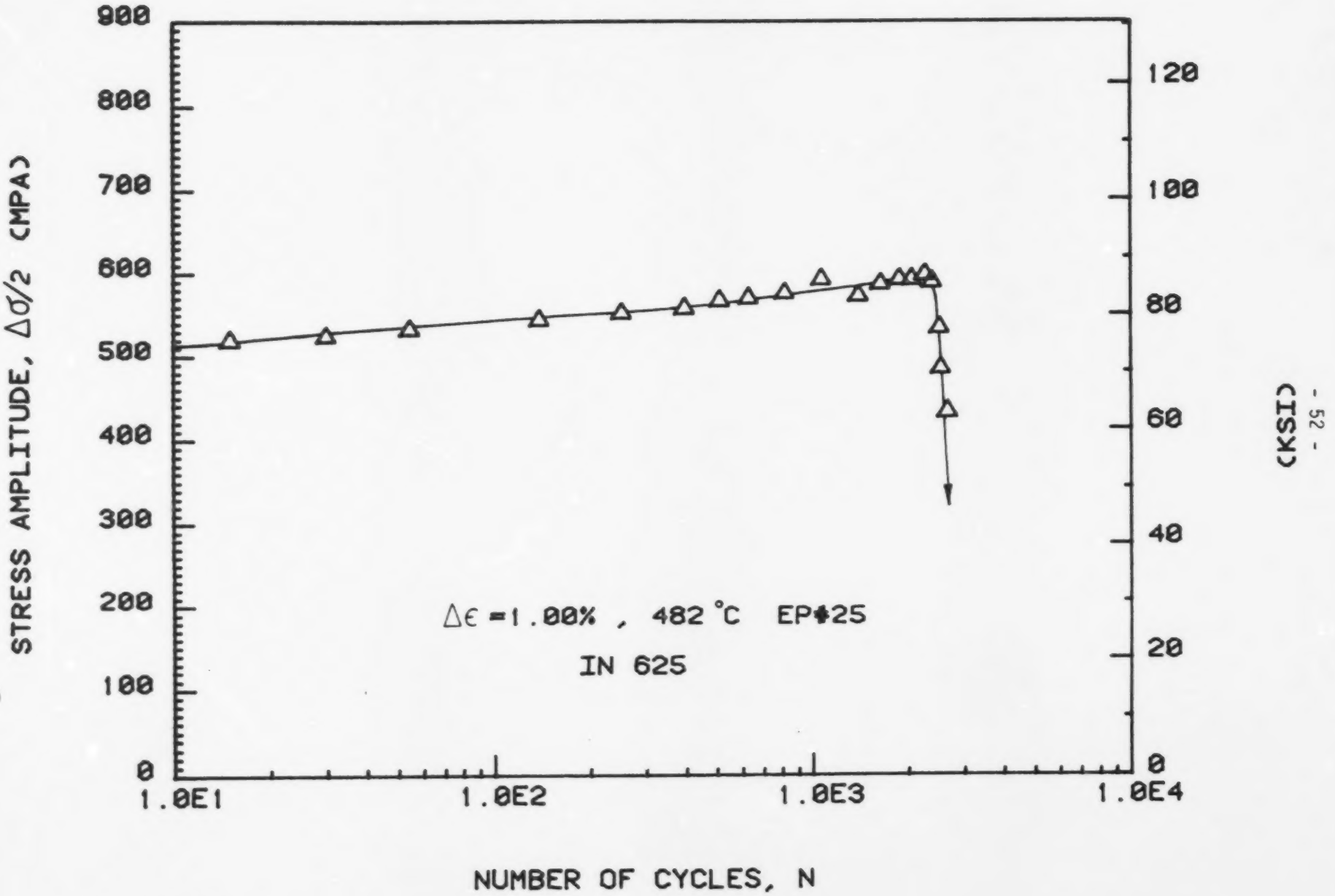
900
800
700
600
500
400
300
200
100
0
120
100
80
60
40
20
0
1.0E1
1.0E2
1.0E3
1.0E4
STRESS AMPLITUDE, Δσ/2 (MPA)
(KSI)
Δε =1.00% , 482 °C EP#25
IN 625
NUMBER OF CYCLES, N

FIG. A.4

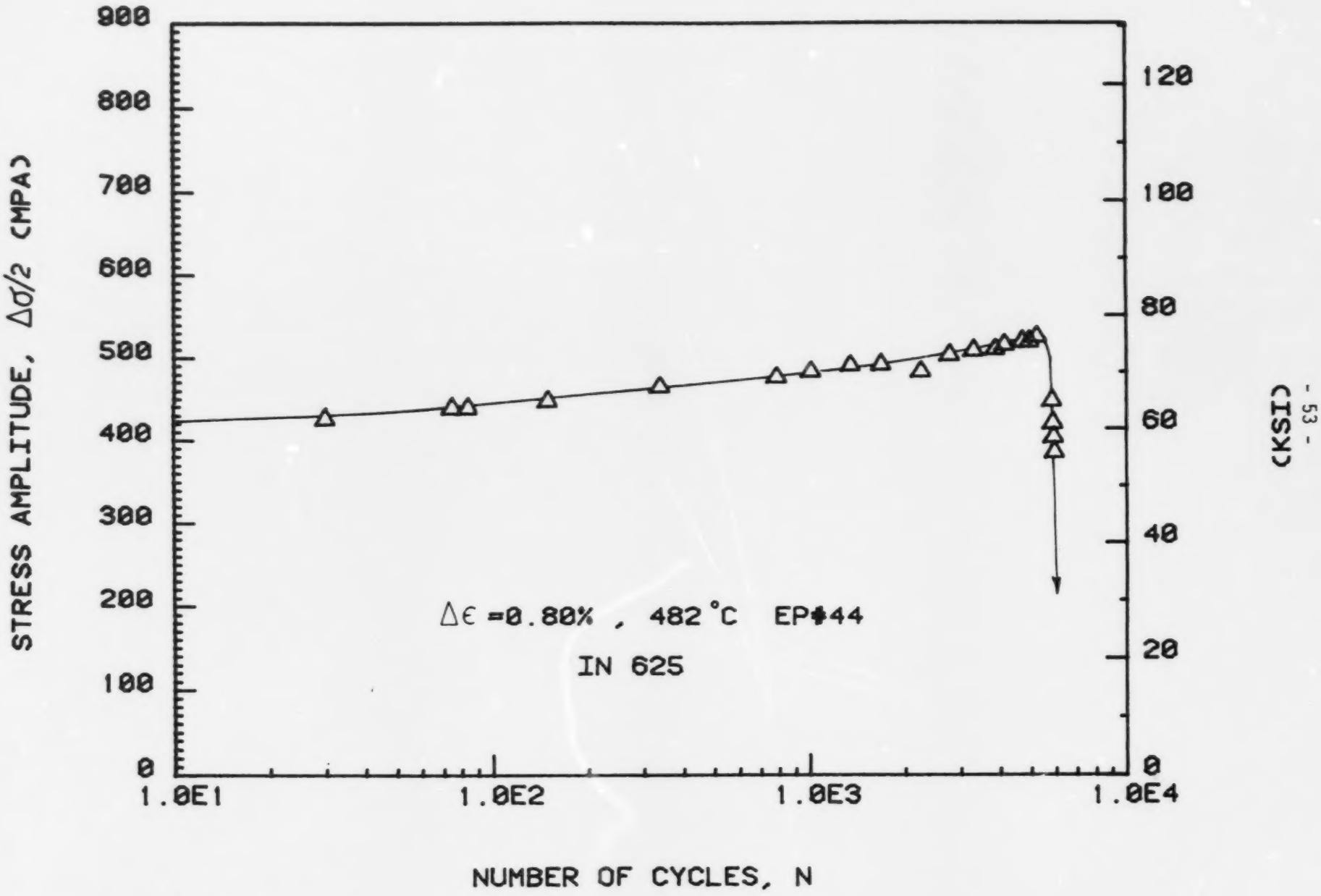
900
800
700
600
500
400
300
200
100
0
STRESS AMPLITUDE, Δσ/2 (MPA)
120
100
80
60
40
20
0
(KSI)
Δε =0.80% , 482 °C EP#44
IN 625
1.0E1
1.0E2
1.0E3
1.0E4
NUMBER OF CYCLES, N

FIG. A.5

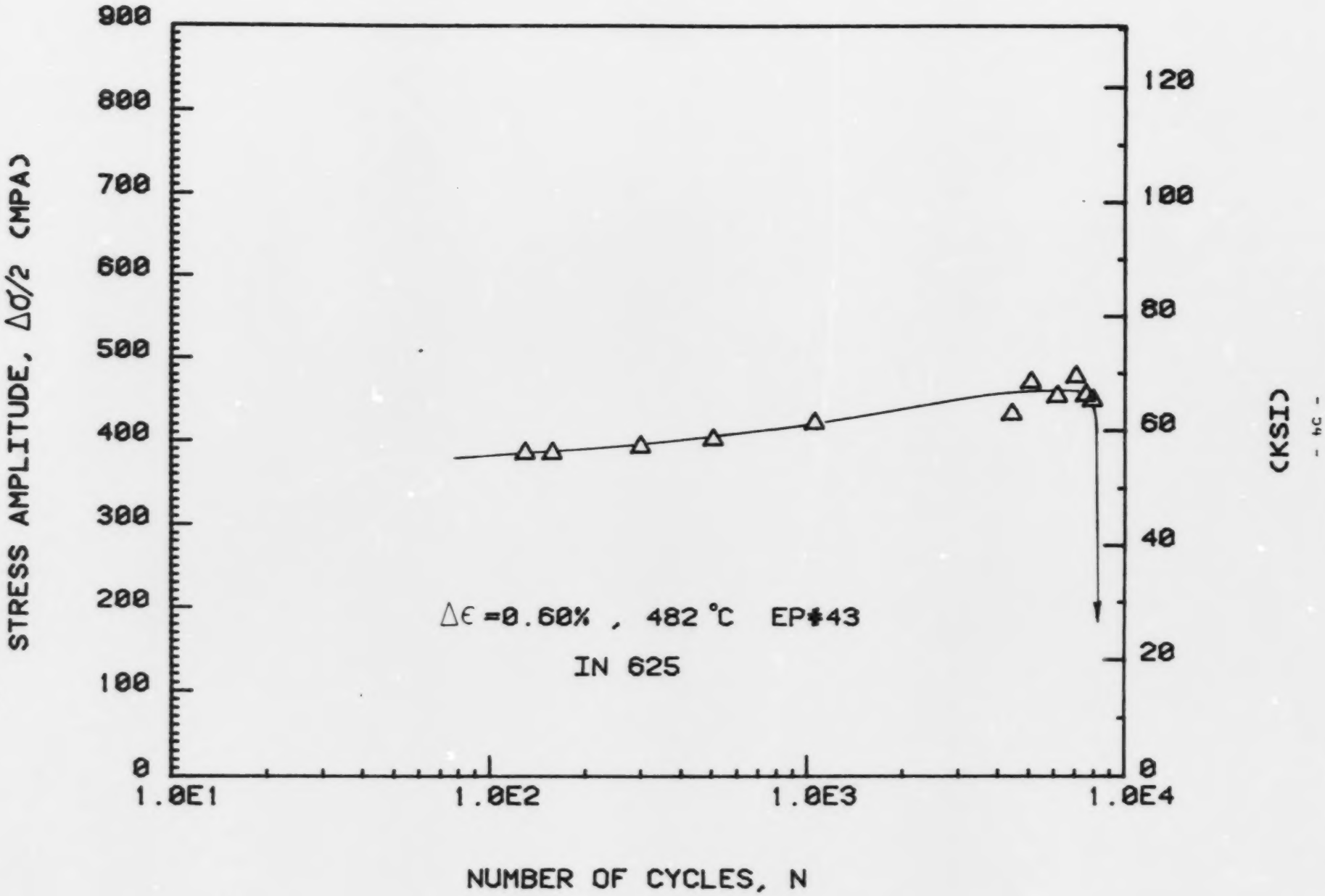
900
800
700
600
500
400
300
200
100
0
120
100
80
60
40
20
0
1.0E1
1.0E2
1.0E3
1.0E4
STRESS AMPLITUDE, Δσ/2 (MPA)
(KSI)
Δε =0.60% , 482 °C EP#43
IN 625
NUMBER OF CYCLES, N

FIG. A.6

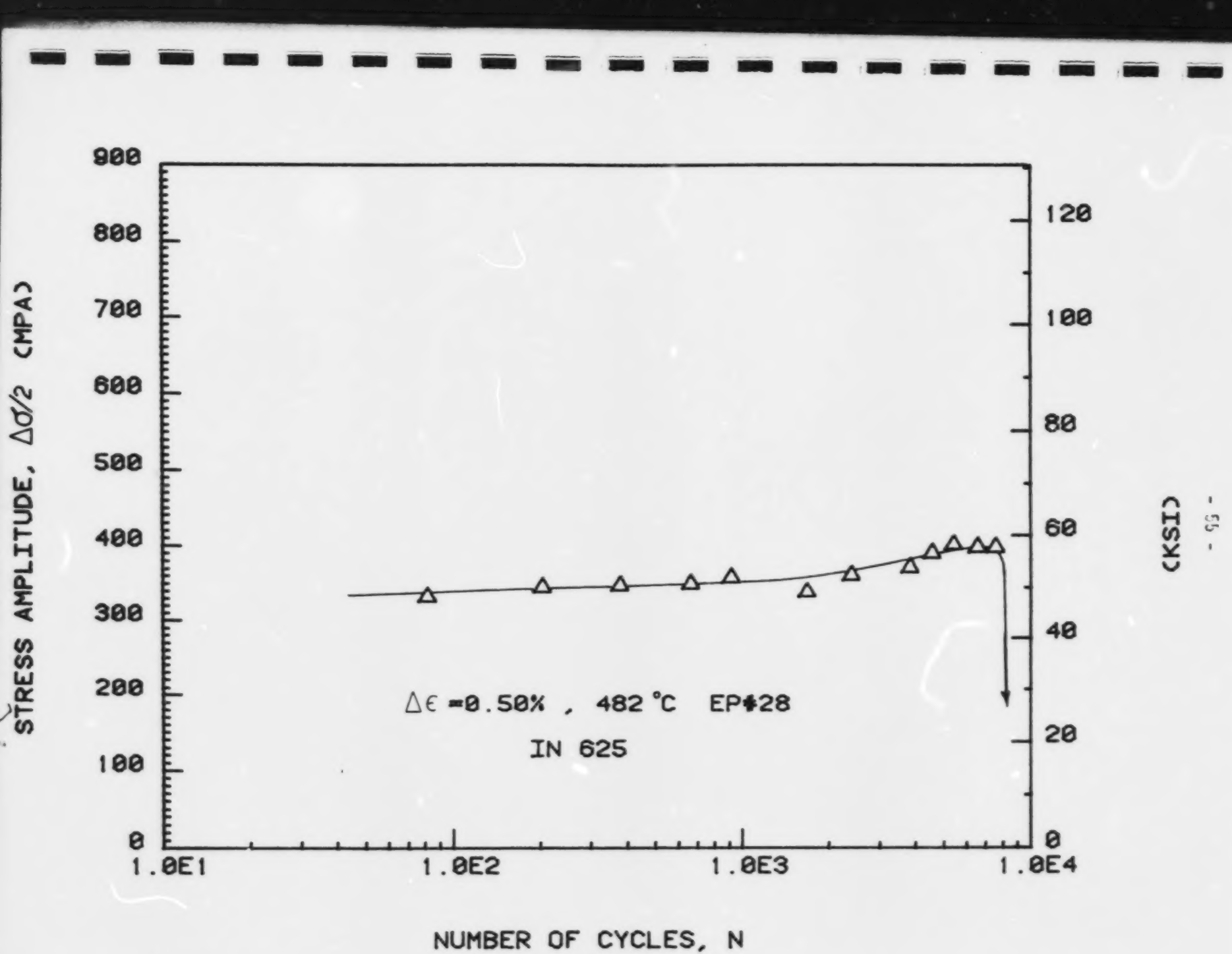
STRESS AMPLITUDE, Δσ/2 (MPA)
900
800
700
600
500
400
300
200
100
0
120
100
80
60
40
20
0
(KSI)
Δε =0.50% , 482 °C EP#28
IN 625
1.0E1
1.0E2
1.0E3
1.0E4
NUMBER OF CYCLES, N

FIG. A.7

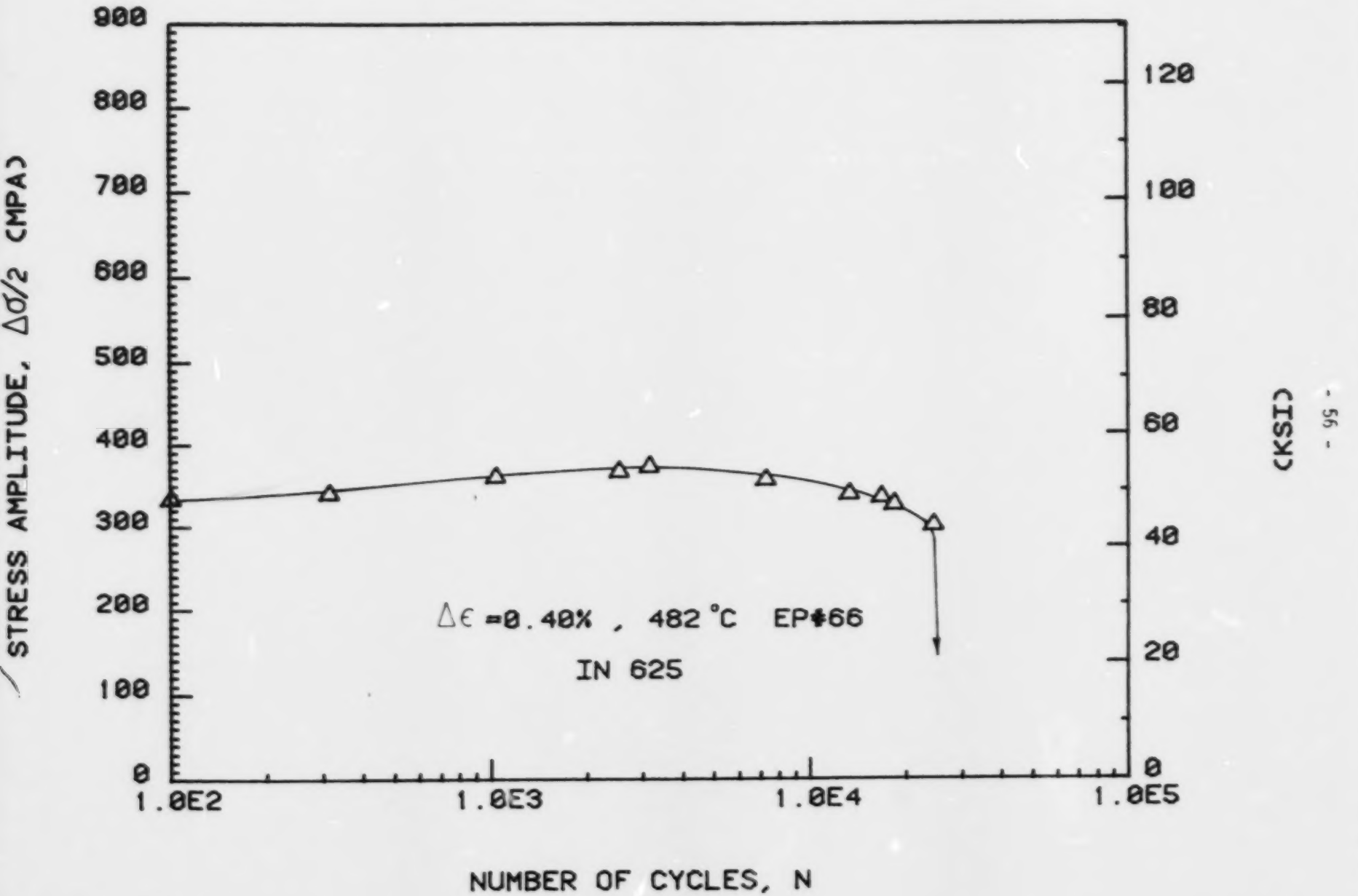
900
800
700
600
500
400
300
200
100
0
120
100
80
60
40
20
0
1.0E2
1.0E3
1.0E4
1.0E5
STRESS AMPLITUDE, Δσ/2 (MPA)
(KSI)
Δε =0.40% , 482 °C EP#66
IN 625
NUMBER OF CYCLES, N

FIG. A.8

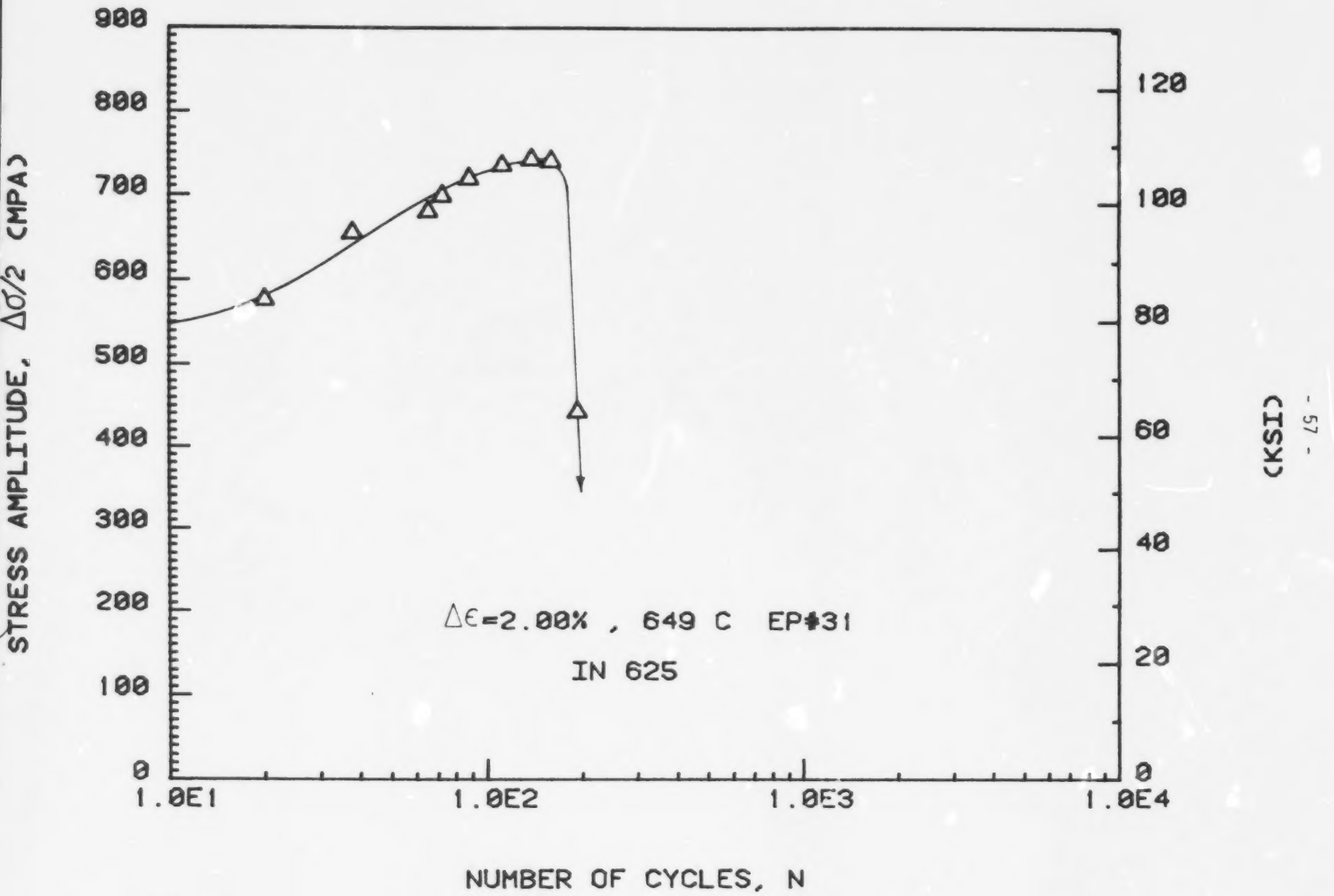
900
800
700
600
500
400
300
200
100
0
120
100
80
60
40
20
0
1.0E1
1.0E2
1.0E3
1.0E4
STRESS AMPLITUDE, Δσ/2 (MPA)
(KSI)
Δε=2.00% , 649 C EP#31
IN 625
NUMBER OF CYCLES, N

FIG. A.9

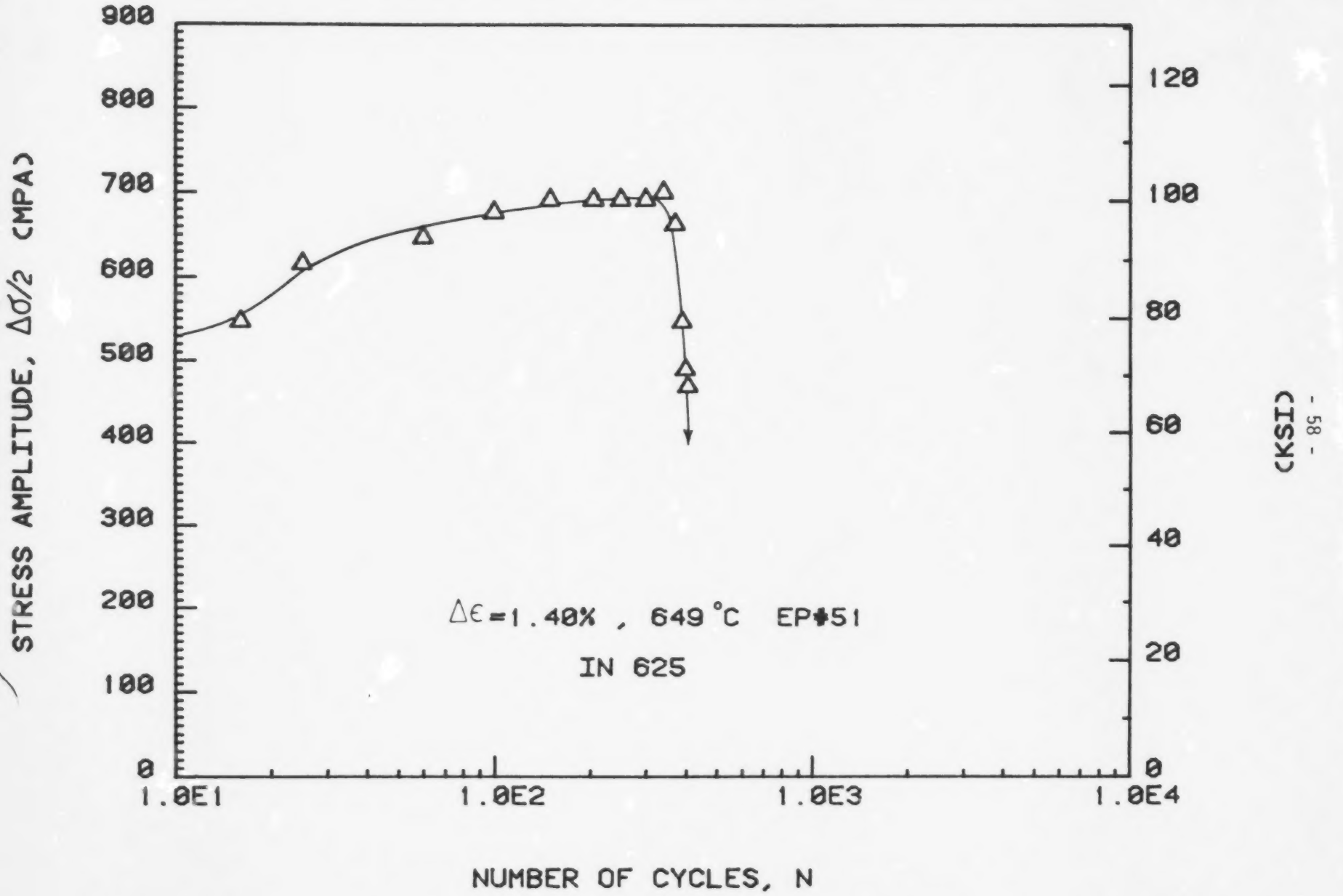
900
800
700
600
500
400
300
200
100
0
120
100
80
60
40
20
0
1.0E1
1.0E2
1.0E3
1.0E4
STRESS AMPLITUDE, Δσ/2 (MPA)
(KSI)
Δε=1.40% , 649 °C EP#51
IN 625
NUMBER OF CYCLES, N

FIG. A.10

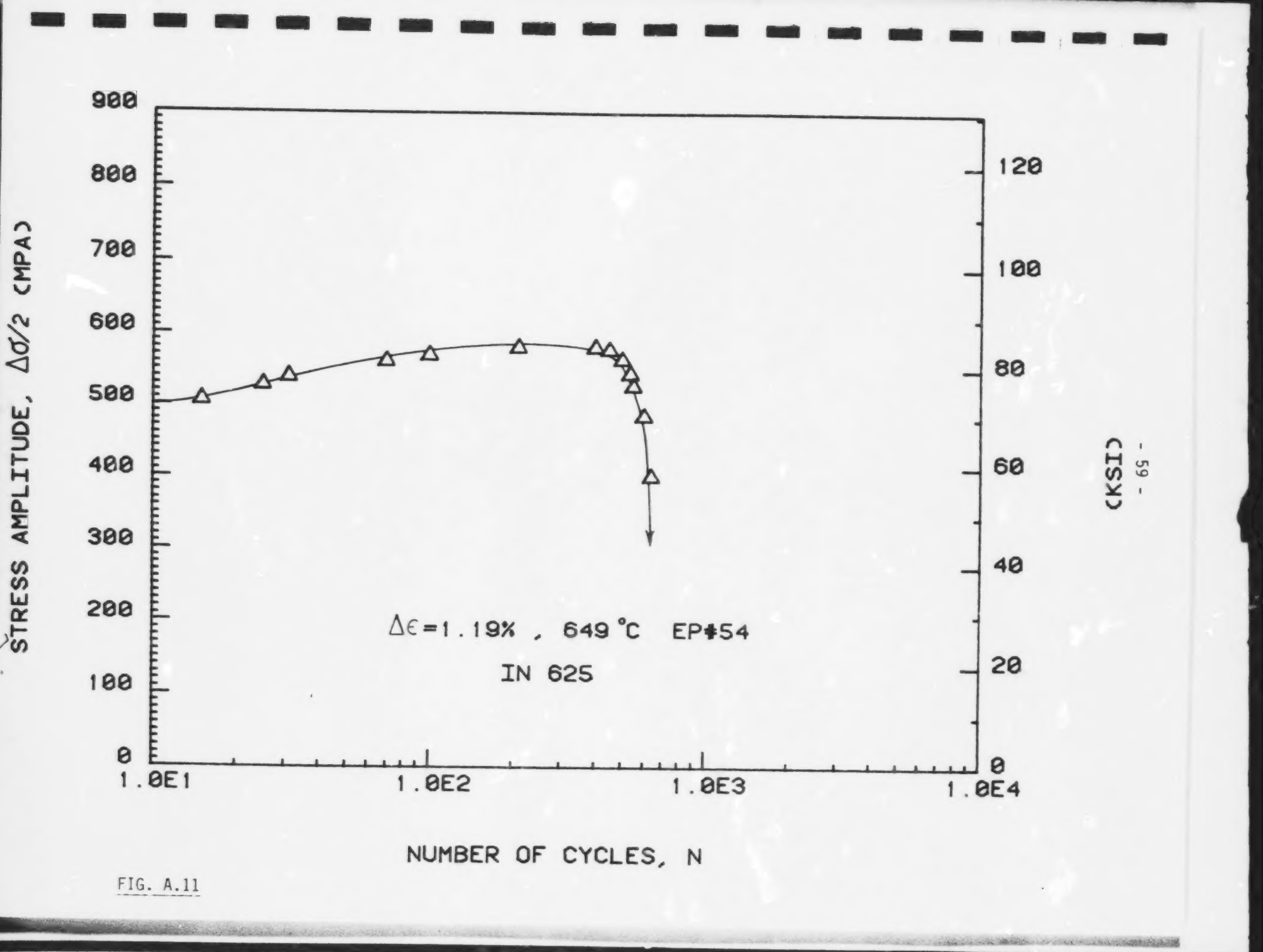
STRESS AMPLITUDE, Δσ/2 (MPA)
900
800
700
600
500
400
300
200
100
0
120
100
80
60
40
20
0
(KSI)
Δε=1.19% , 649 °C EP#54
IN 625
1.0E1
1.0E2
1.0E3
1.0E4
NUMBER OF CYCLES, N

FIG. A.11

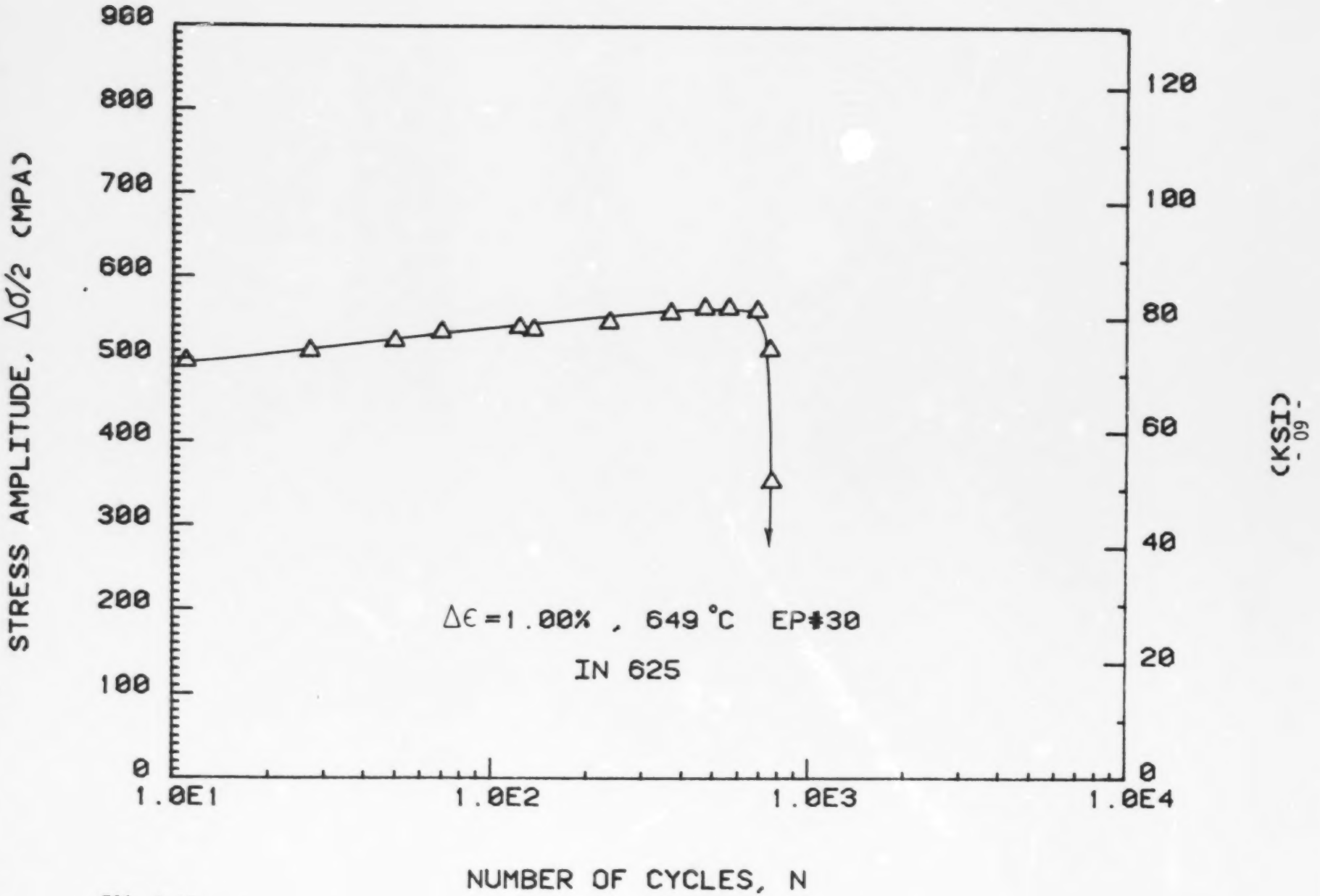
900
800
700
600
500
400
300
200
100
0
120
100
80
60
40
20
0
1.0E1
1.0E2
1.0E3
1.0E4
STRESS AMPLITUDE, Δσ/2 (MPA)
(KSI)
Δε=1.00% , 649 °C EP#30
IN 625
NUMBER OF CYCLES, N

FIG. A.12

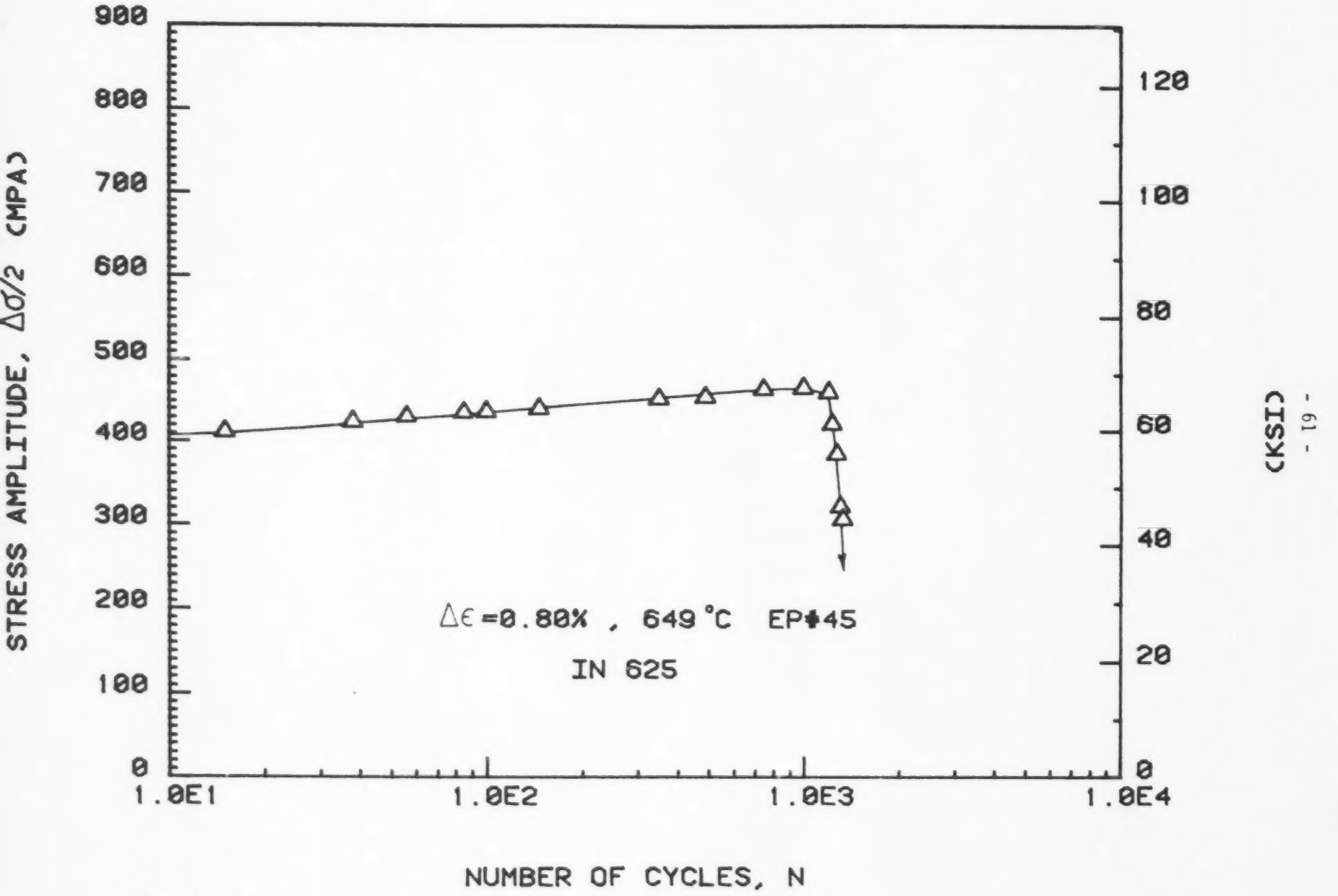
900
800
700
600
500
400
300
200
100
0
STRESS AMPLITUDE, Δσ/2 (MPA)
120
100
80
60
40
20
0
(KSI)
1.0E1
1.0E2
1.0E3
1.0E4
Δε=0.80% , 649°C EP#45
IN 625
NUMBER OF CYCLES, N

FIG. A.13

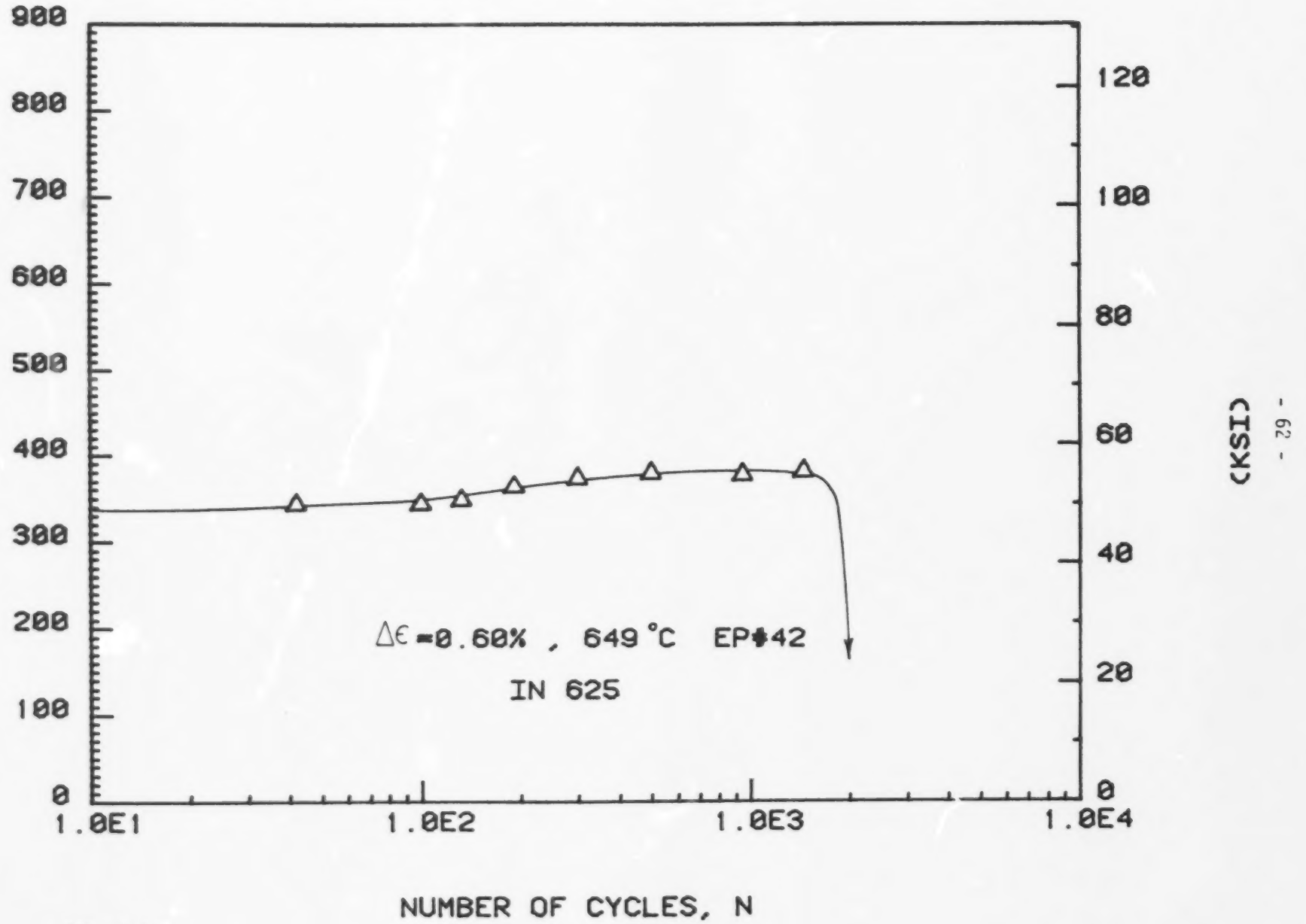
900
800
700
600
500
400
300
200
100
0
120
100
80
60
40
20
0
1.0E1
1.0E2
1.0E3
1.0E4
STRESS AMPLITUDE, Δσ/2 (MPA)
(KSI)
Δε=0.60% , 649 °C EP#42
IN 625
NUMBER OF CYCLES, N

FIG. A.14

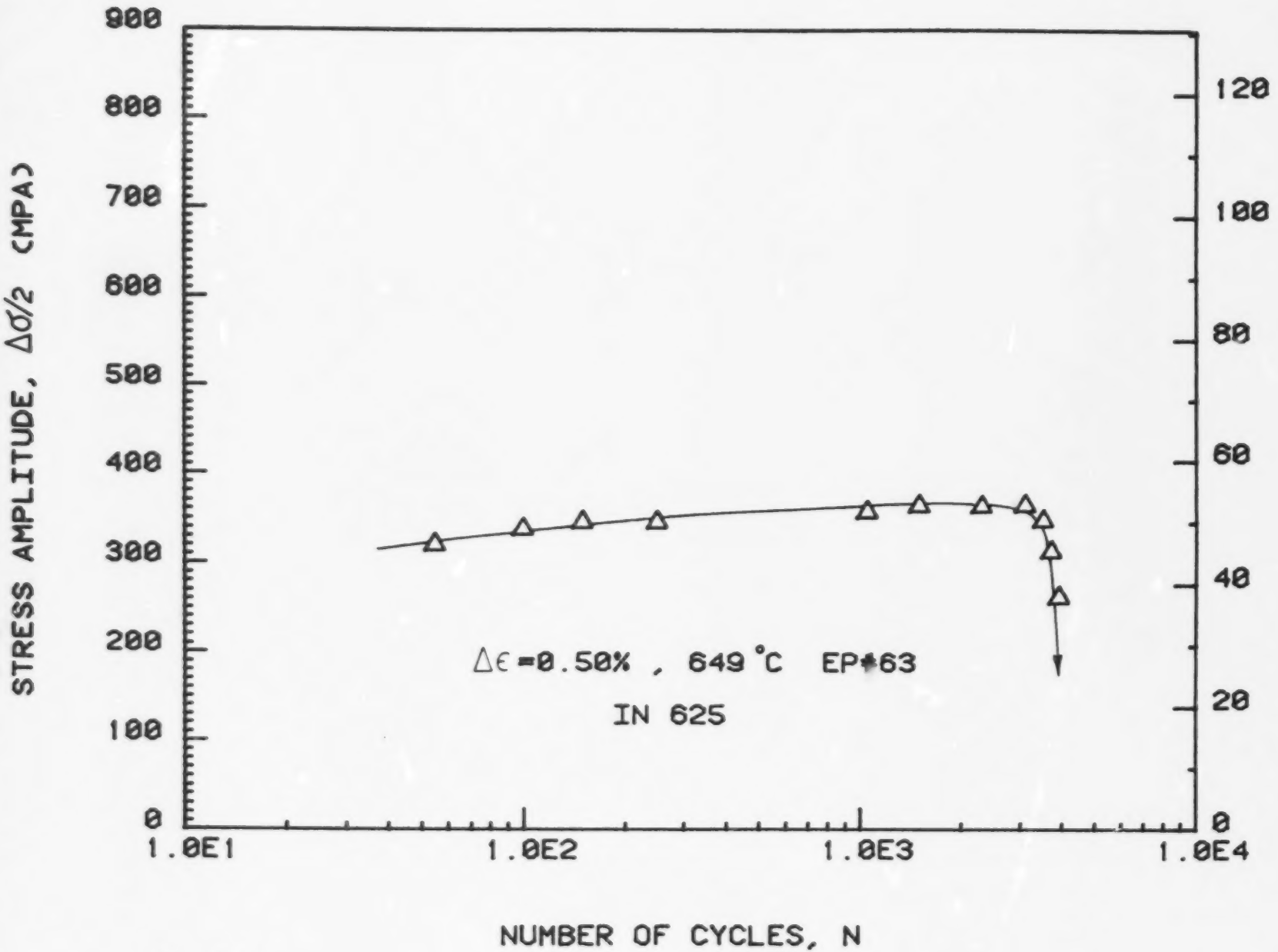
900
800
700
600
500
400
300
200
100
0
1.0E1
1.0E2
1.0E3
1.0E4
120
100
80
60
40
20
0
STRESS AMPLITUDE, Δσ/2 (MPA)
(KSI)
Δε=0.50% , 649 °C EP#63
IN 625
NUMBER OF CYCLES, N

FIG. A.15

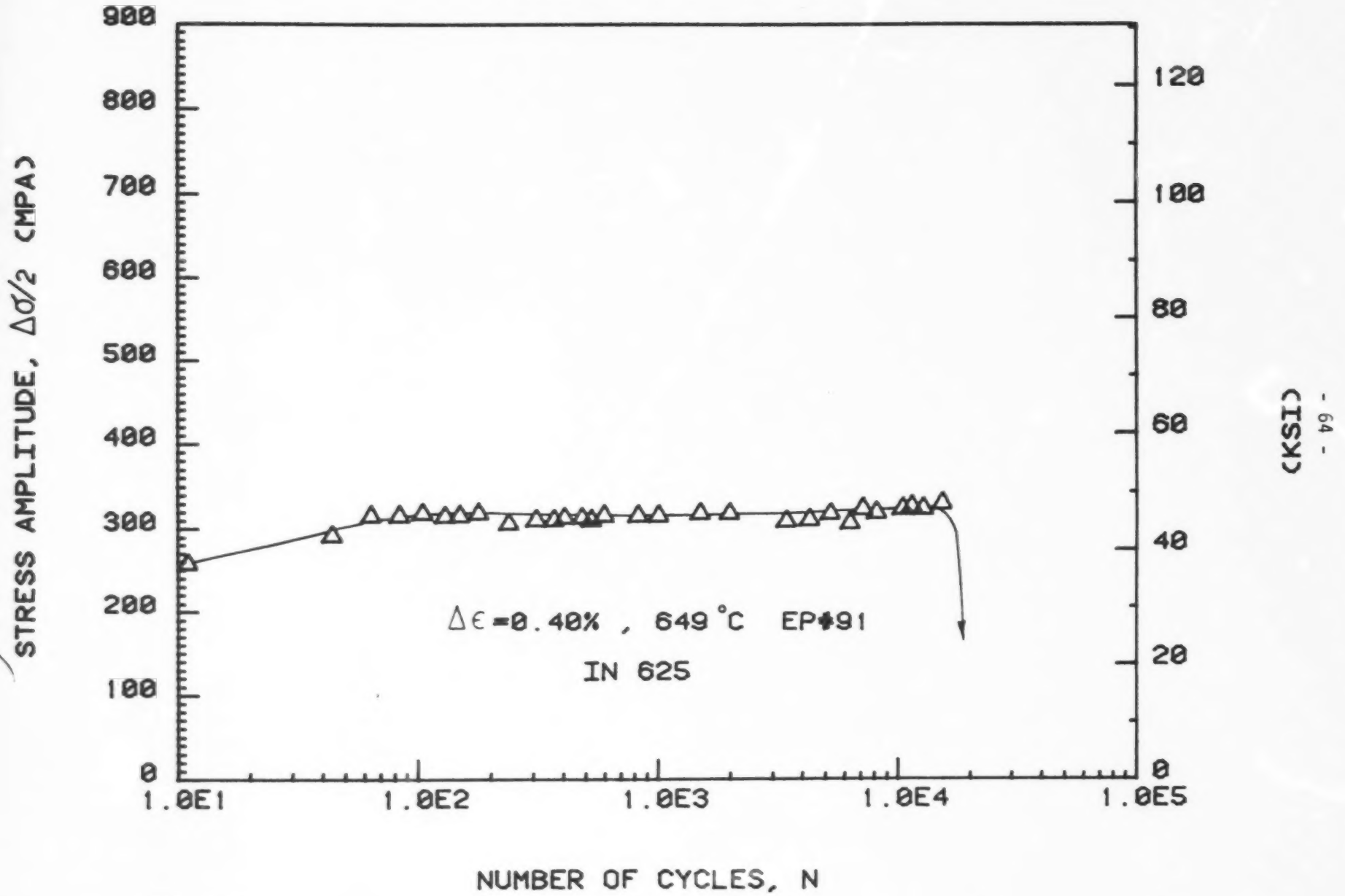
900
800
700
600
500
400
300
200
100
0
STRESS AMPLITUDE, Δσ/2 (MPA)
120
100
80
60
40
20
0
(KSI)
Δε=0.40% , 649 °C EP#91
IN 625
1.0E1
1.0E2
1.0E3
1.0E4
1.0E5
NUMBER OF CYCLES, N

FIG. A.16

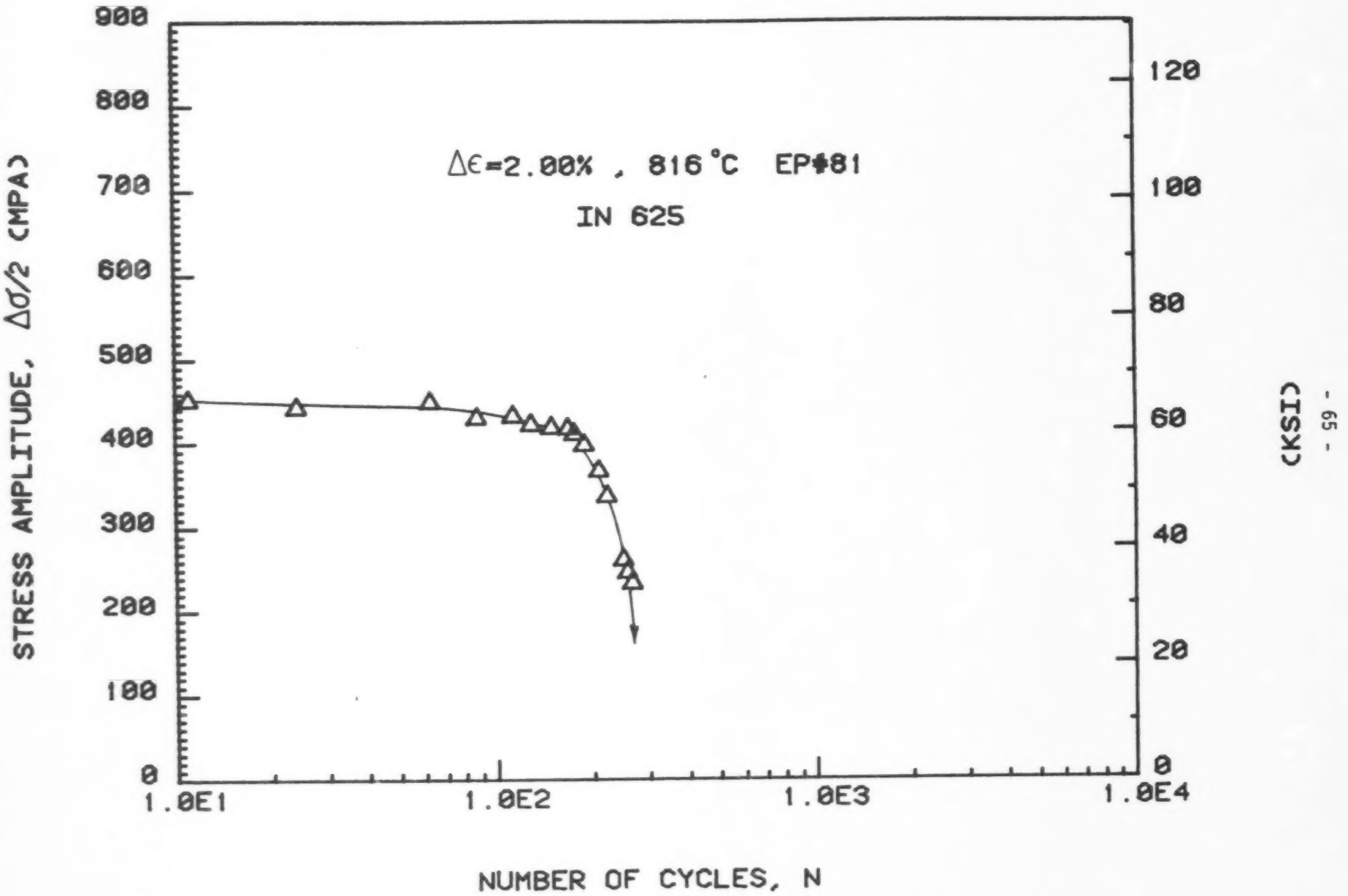
Δε=2.00% , 816°C EP#81
IN 625
STRESS AMPLITUDE, Δσ/2 (MPA)
(KSI)
NUMBER OF CYCLES, N
900
800
700
600
500
400
300
200
100
0
120
100
80
60
40
20
0
1.0E1
1.0E2
1.0E3
1.0E4

FIG. A.17

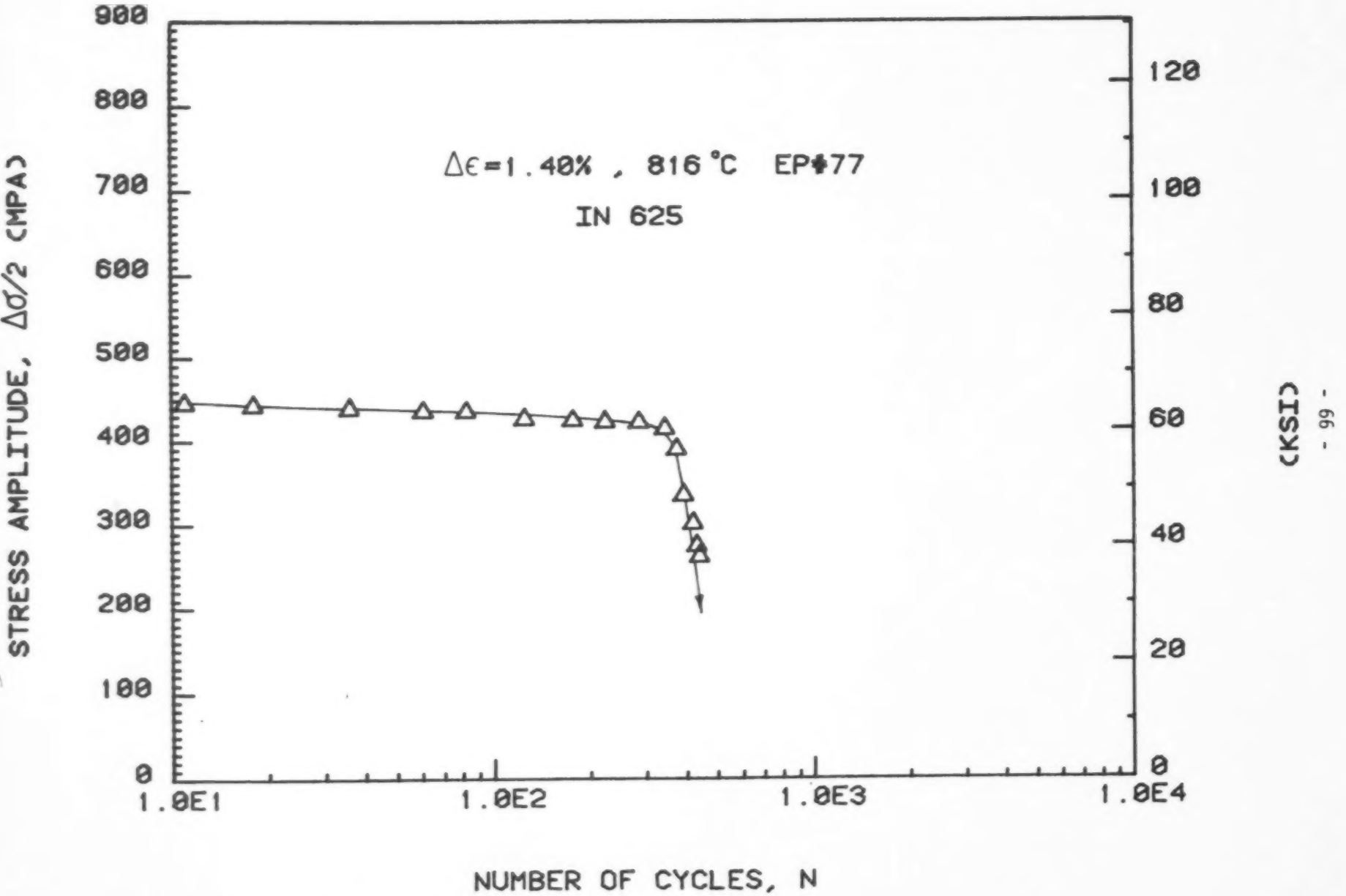
Δε=1.40% , 816 °C EP#77
IN 625
STRESS AMPLITUDE, Δσ/2 (MPA)
(KSI)
NUMBER OF CYCLES, N
900
800
700
600
500
400
300
200
100
0
120
100
80
60
40
20
0
1.0E1
1.0E2
1.0E3
1.0E4

FIG. A.18

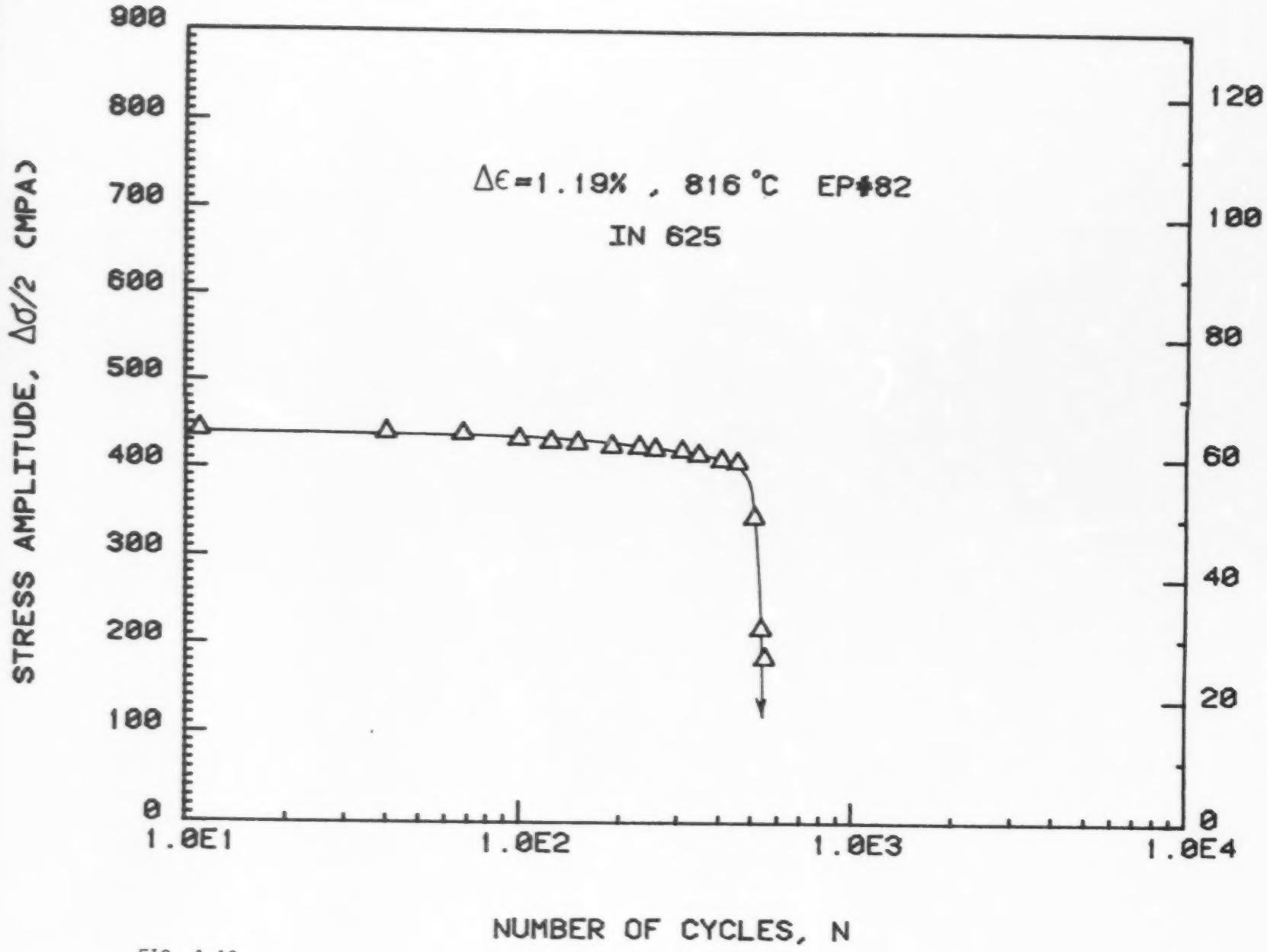
Δε=1.19% , 816 °C EP#82
IN 625
STRESS AMPLITUDE, Δσ/2 (MPA)
(KSI)
NUMBER OF CYCLES, N
900
800
700
600
500
400
300
200
100
0
120
100
80
60
40
20
0
1.0E1
1.0E2
1.0E3
1.0E4

FIG. A.19

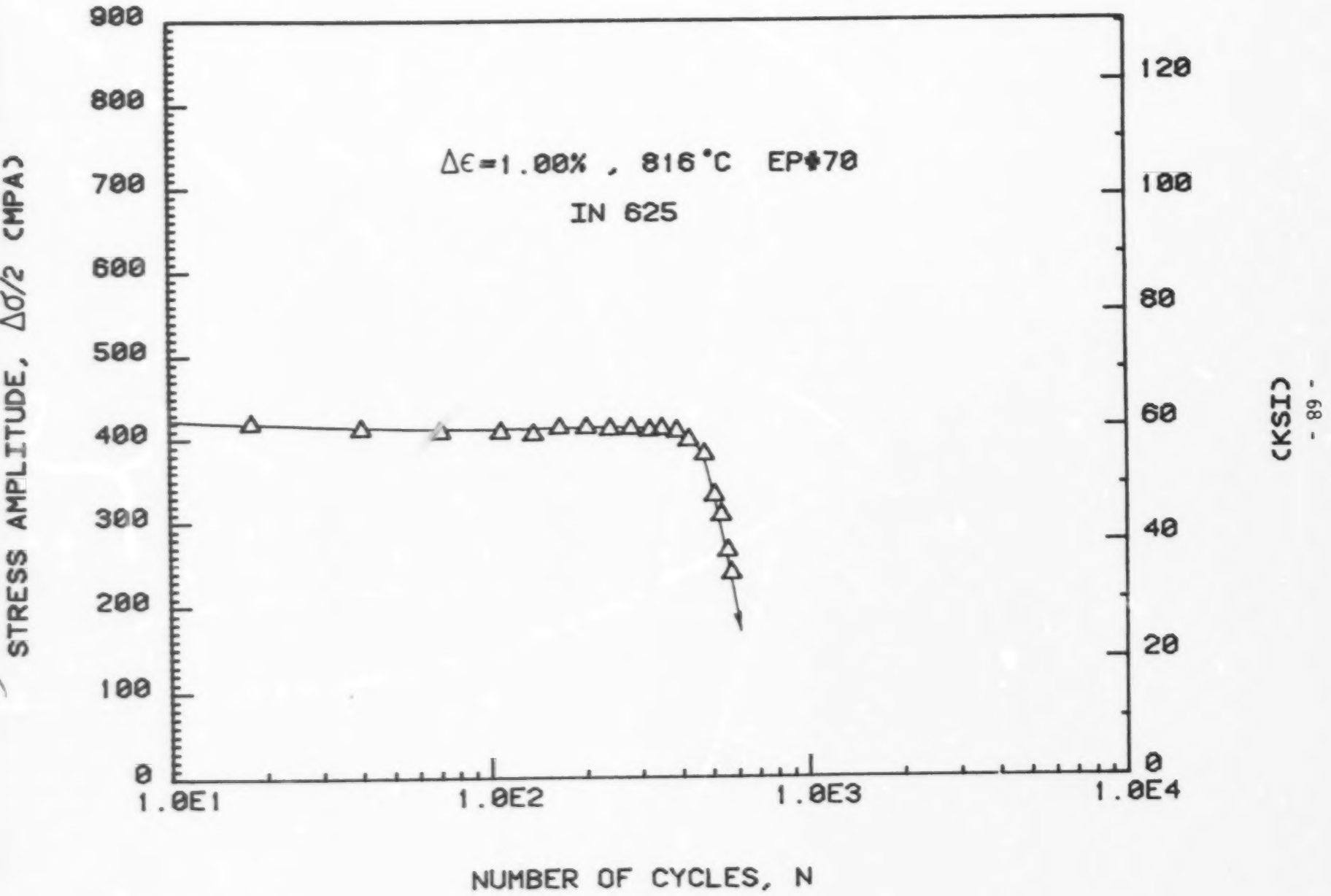
Δε=1.00% , 816°C EP#70
IN 625
STRESS AMPLITUDE, Δσ/2 (MPA)
900
800
700
600
500
400
300
200
100
0
120
100
80
60
40
20
0
(KSI)
1.0E1
1.0E2
1.0E3
1.0E4
NUMBER OF CYCLES, N

FIG. A.20

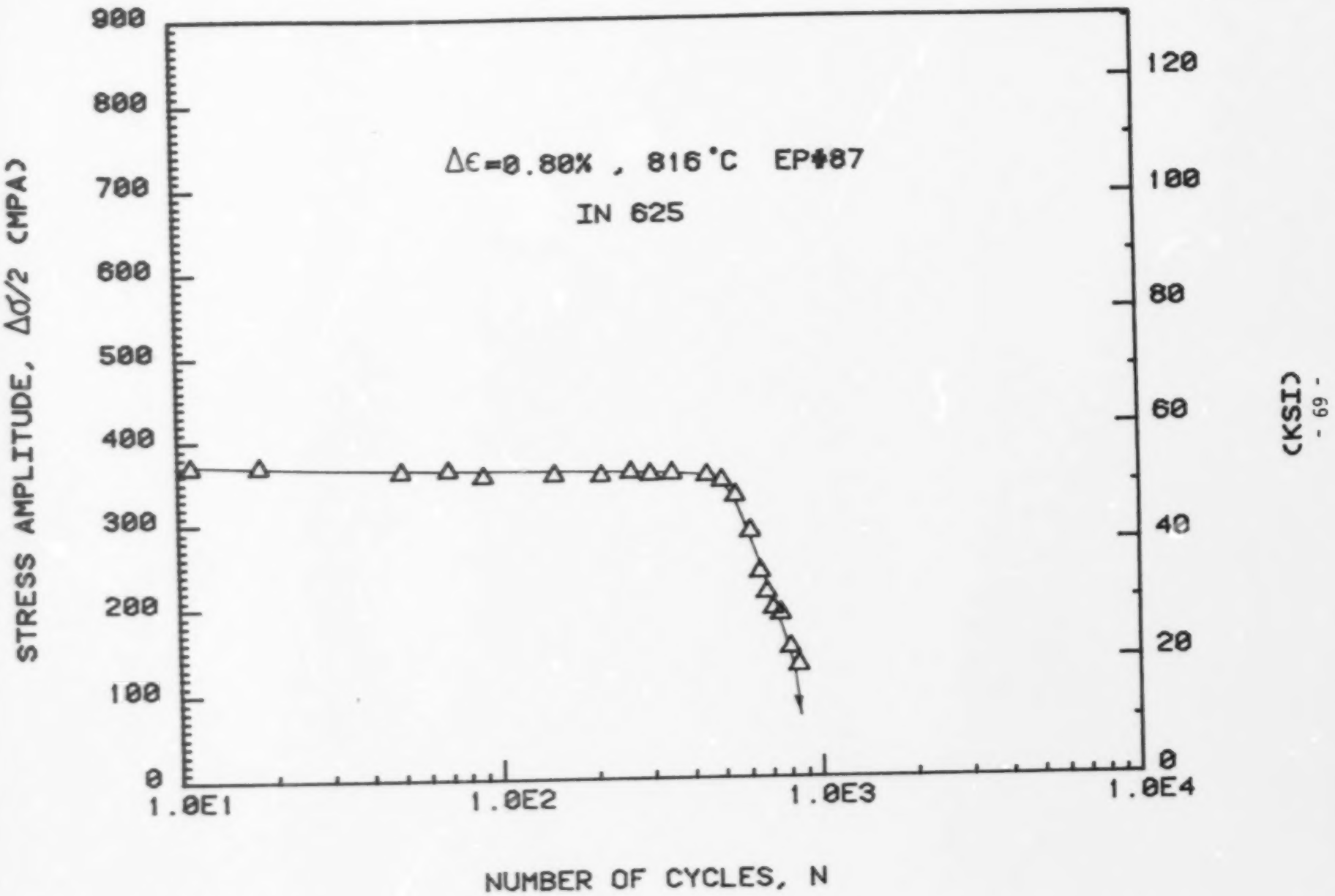
Δε=0.80% , 816°C EP#87
IN 625
STRESS AMPLITUDE, Δσ/2 (MPA)
900
800
700
600
500
400
300
200
100
0
120
100
80
60
40
20
0
(KSI)
1.0E1
1.0E2
1.0E3
1.0E4
NUMBER OF CYCLES, N

FIG. A.21

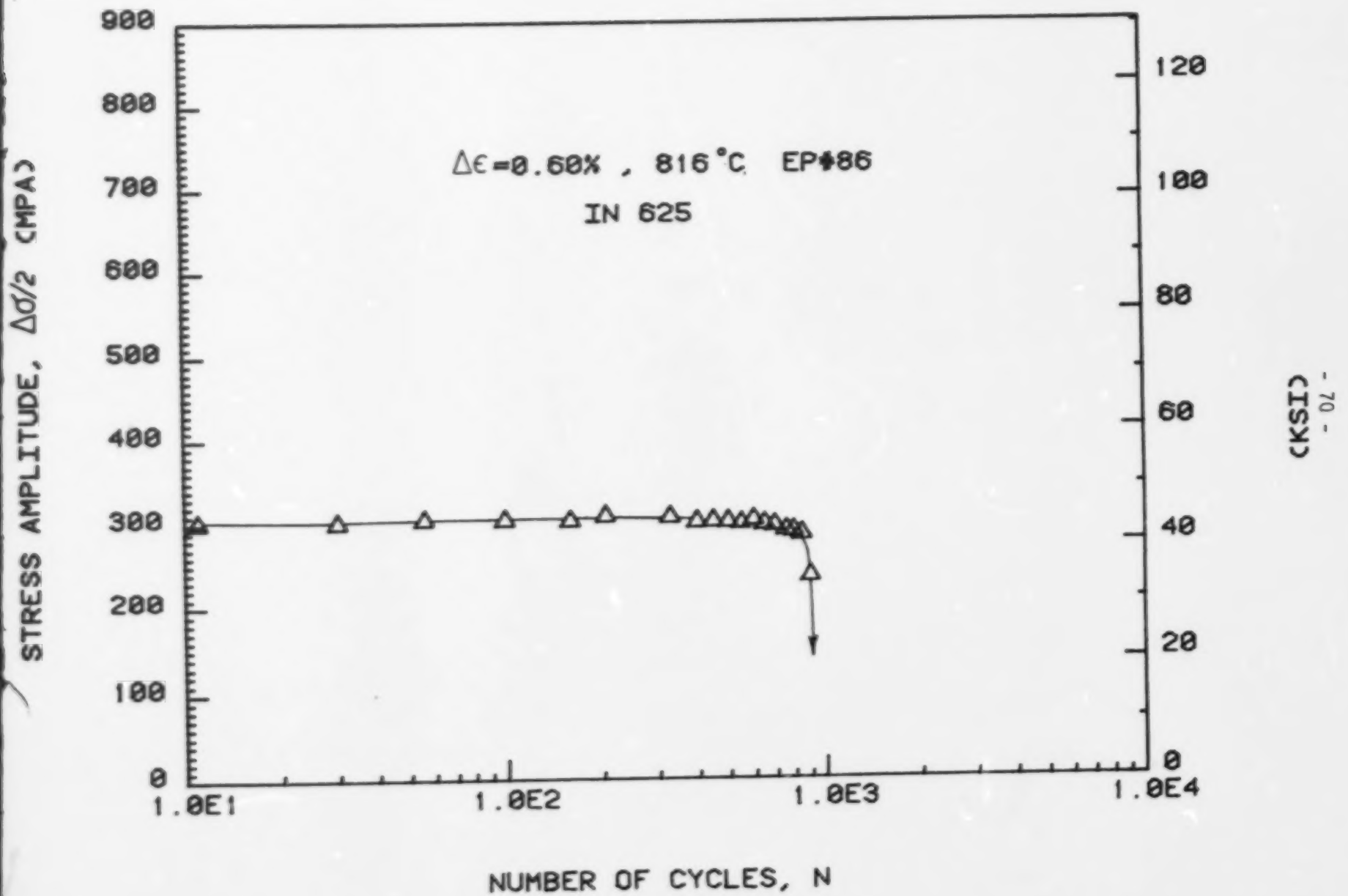
Δε=0.60% , 816°C EP#86
IN 625
STRESS AMPLITUDE, Δσ/2 (MPA)
(KSI)
NUMBER OF CYCLES, N
900
800
700
600
500
400
300
200
100
0
120
100
80
60
40
20
0
1.0E1
1.0E2
1.0E3
1.0E4

FIG. A.22

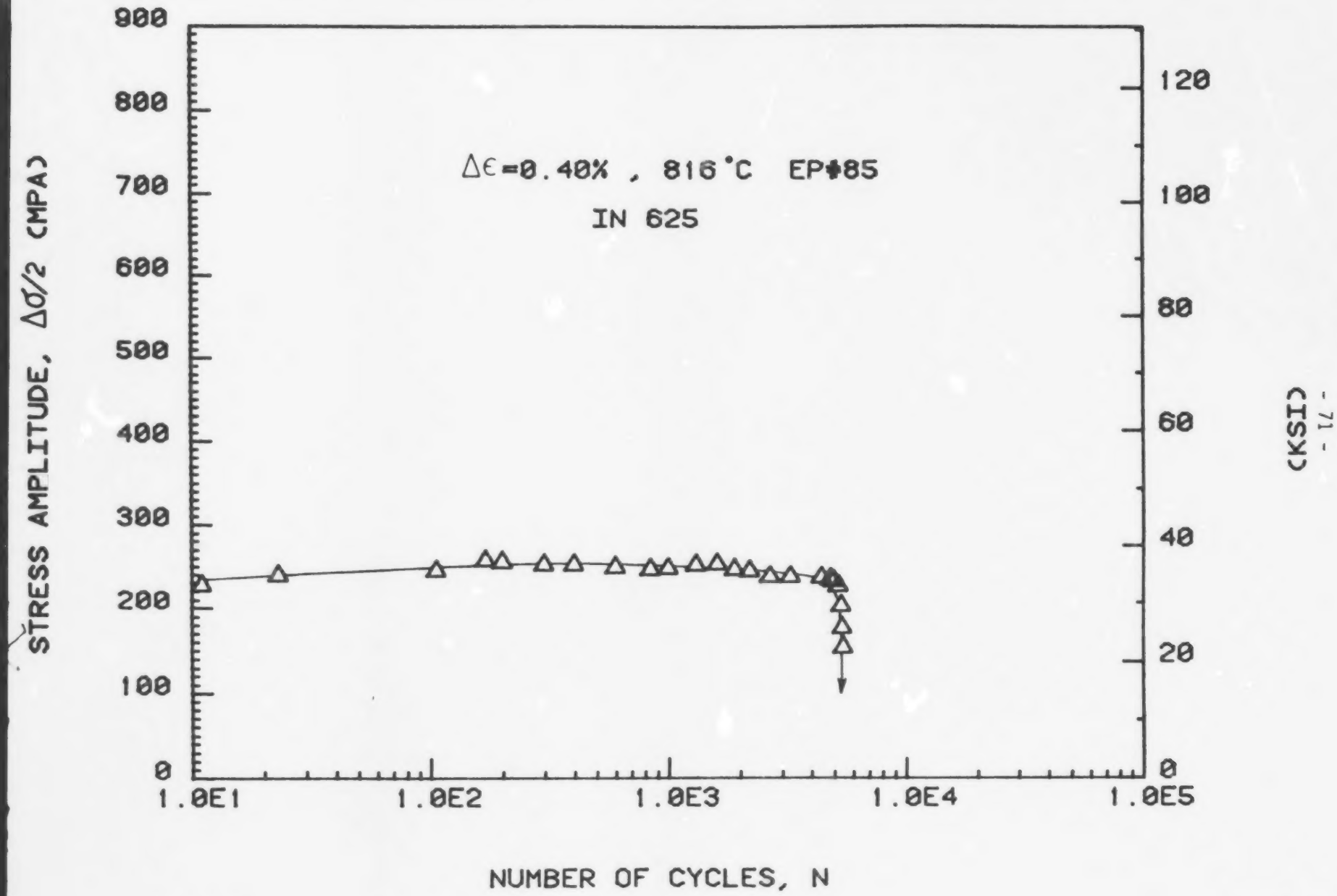
Δε=0.40% , 816°C EP#85
IN 625
STRESS AMPLITUDE, Δσ/2 (MPA)
(KSI)
NUMBER OF CYCLES, N
900
800
700
600
500
400
300
200
100
0
120
100
80
60
40
20
0
1.0E1
1.0E2
1.0E3
1.0E4
1.0E5

FIG. A.23